Turbidity currents interacting with three-dimensional seafloor topographies: A depth-resolved numerical investigation

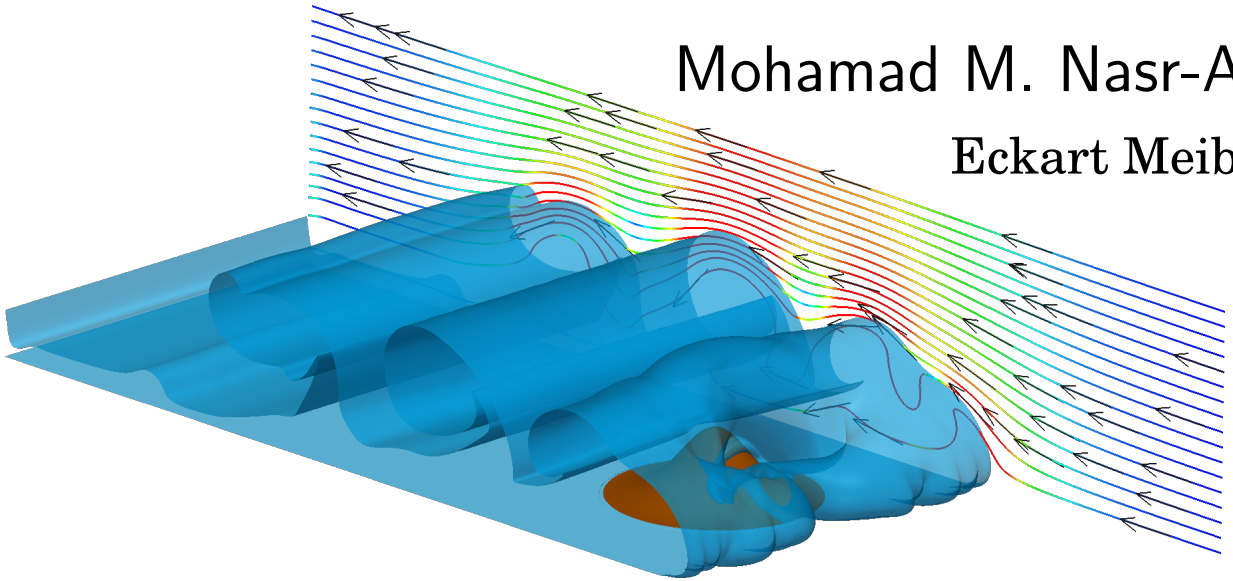

Mohamad M. Nasr-Azadani

Eckart Meiburg

UC SANTA BARBARA engineering

What is a turbidity current?

- A special class of gravity current
- Form due to hydrostatic pressure gradient
- Density difference: Temperature gradients, salinity, **particles**

Gravity currents: Sandstorms

Sandstorm in Phoenix AZ. Courtesy of Andrew Pielage (http://apizm.com/)

Gravity currents: Powdersnow avalanche

Avalanche in Mt. Logan in Canada. Courtesy of Jeffrey Levison

Gravity currents: Pyroclastic flows

Left: Mount Pinatubo's eruption (Philippines) in 1991 (Photo by Alberto Garcia/Corbis available at http://www.guardian.co.uk/)
Right: Mount Merapi in central Java, Indonesia (AP Photo, available at http://www.commercialappeal.com/).

Turbidity currents: "Underwater avalanche"

Los Cabos in Baja California, Mexico. Movie by Andre Frota available at http://www.youtube.com/watch?v=ruC77oiGIiE

Turbidity currents

- Front speed: $\mathcal{O}(10)$ m/s
- Front height: $\mathcal{O}(100)$ m
- Travel up to: $\mathcal{O}(1,000)$ km
- Transport $\mathcal{O}(100)$ km^3 sediment

http://www.clas.ufl.edu/

Turbidity currents: the 1929 Grand Banks landslide

7.2 scale earthquake triggered a landslide

Transported $O(200)\ \mathrm{km}^3$ sediment into deep-sea regions ($\approx 800\ \mathrm{km}$)

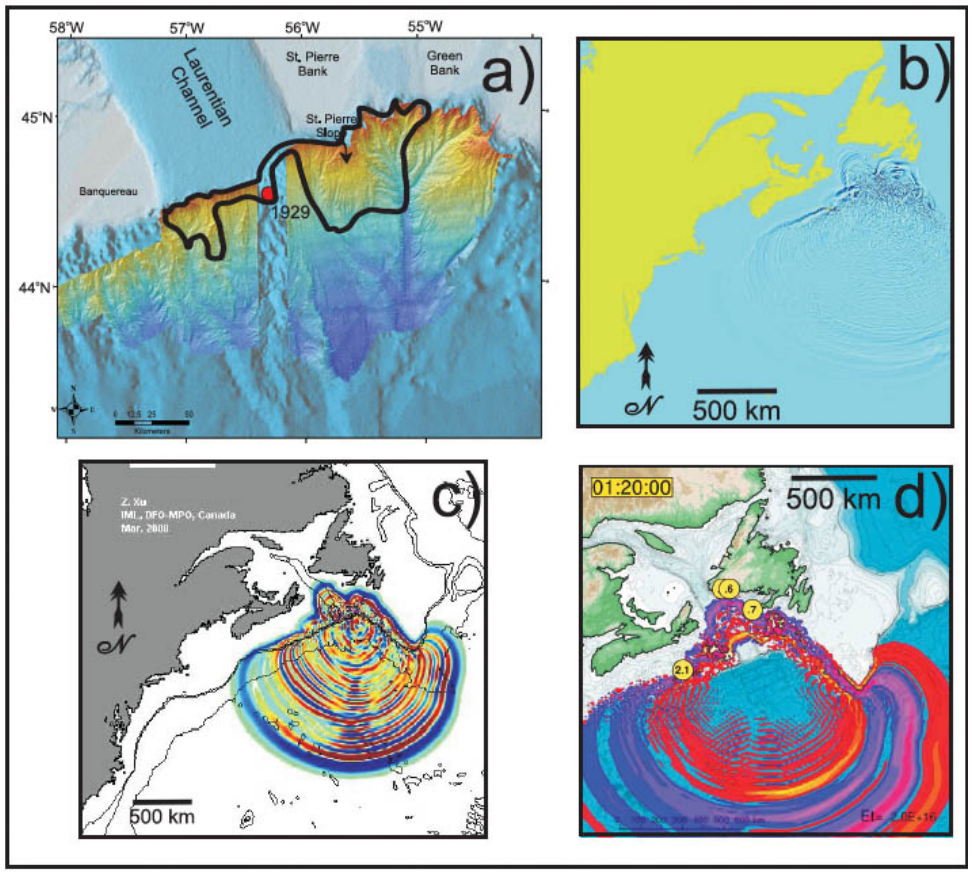

http://journals.hil.unb.ca/ocean

Turbidity currents: the 1929 Grand Banks landslide

Estimated velocity $\approx 15 - 50$ mph (Heezen & Ewing (1952))

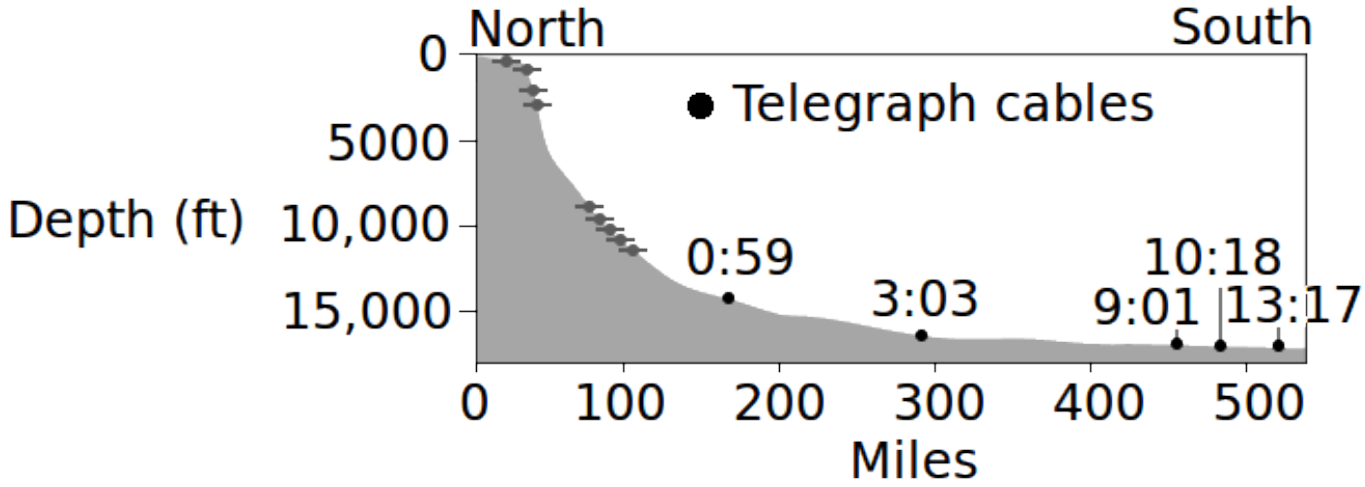

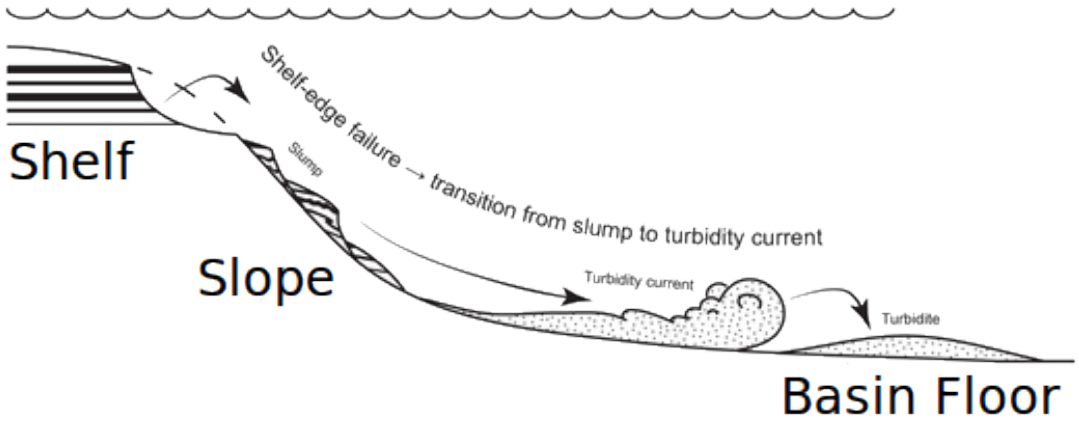

Top: Recorded times (hr:min) of disrupted telegraphs after the 1929 Grand Banks landslide (http://www.geol.lsu.edu/jlorenzo/

Bottom: Configuration of a turbidity current caused by a landslide (Covaul (2011) Nature.)

Motivation

- Transport of sediment from shallow water regions into the deep-sea

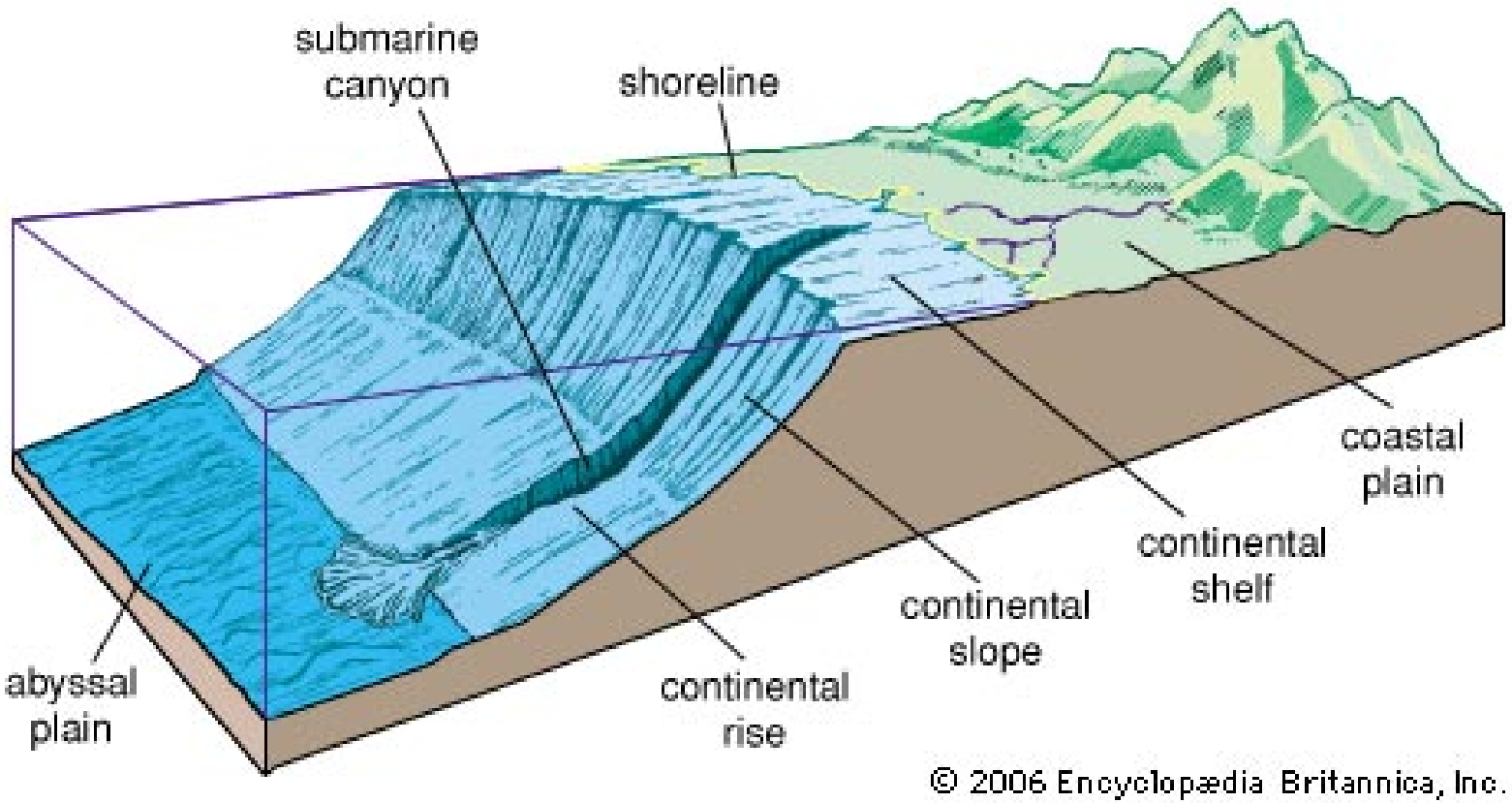

Motivation

- Formation of various topographical features

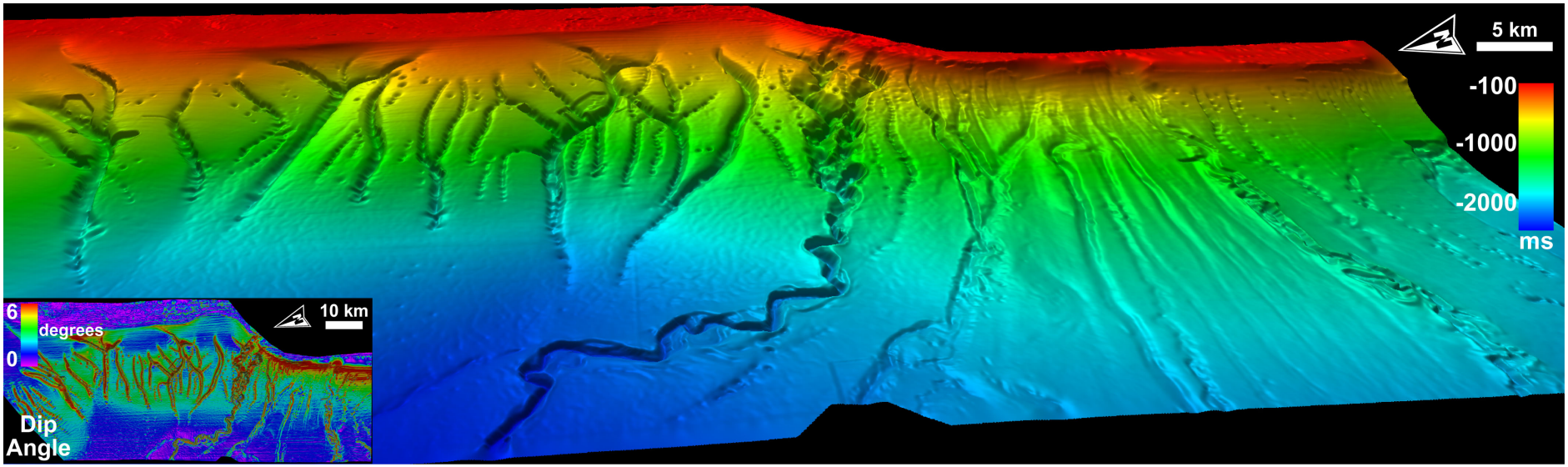

Modern Equatorial Guinean seafloor (http://see-atlas.leeds.ac.uk)

Motivation

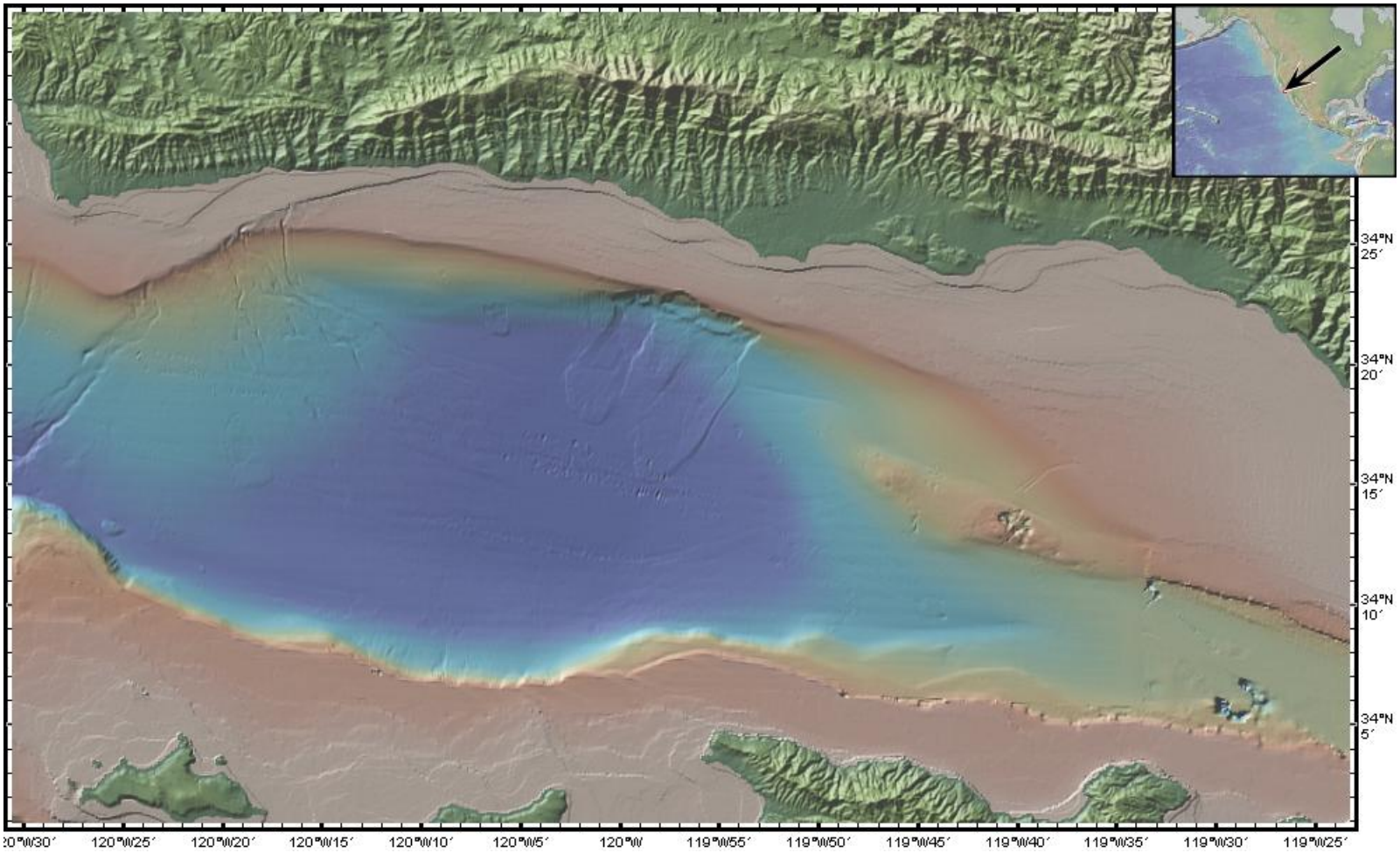

Santa Barbara channel (http://www.mbari.org/)

Motivation

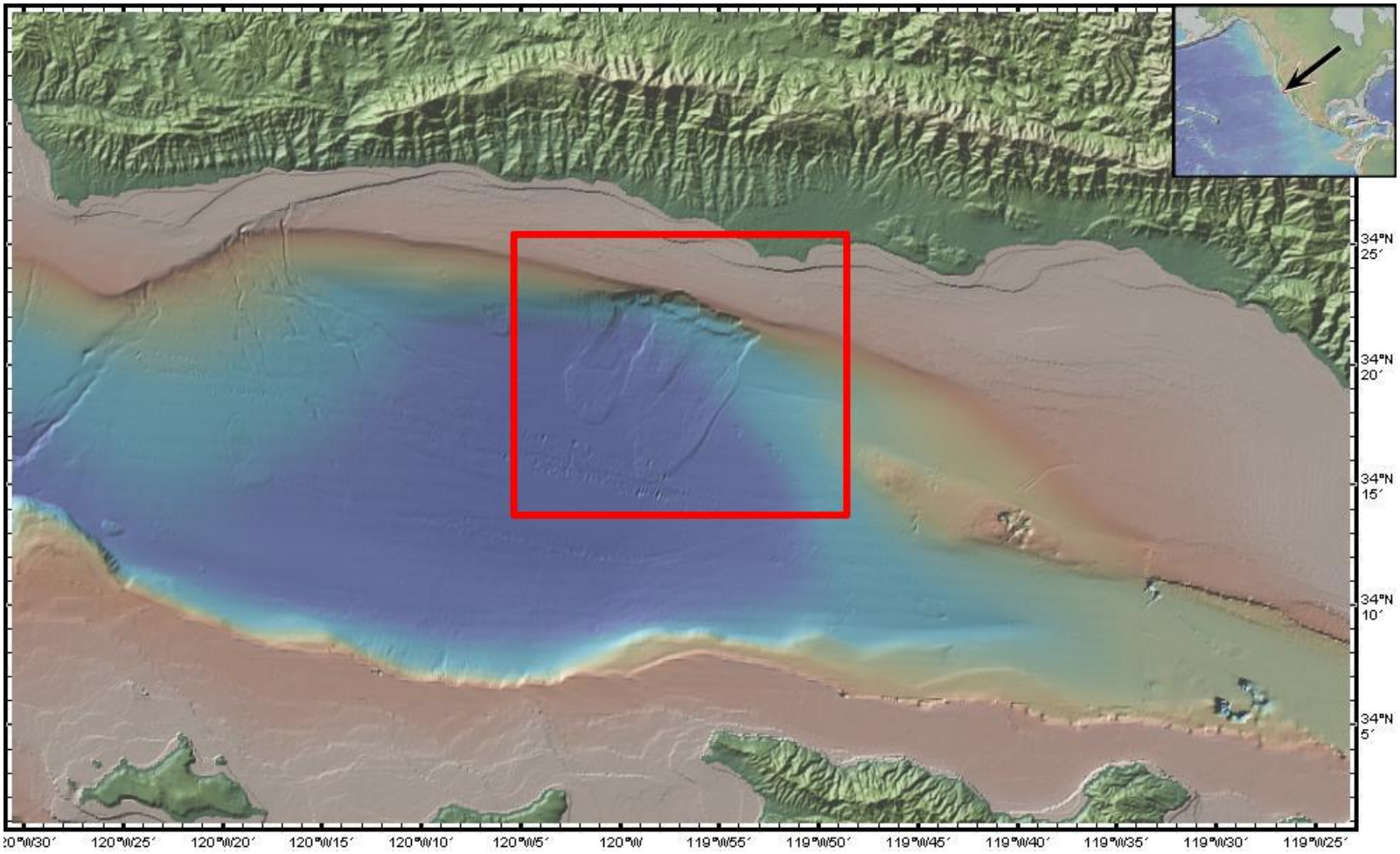

Santa Barbara channel (http://www.mbari.org/)

Motivation

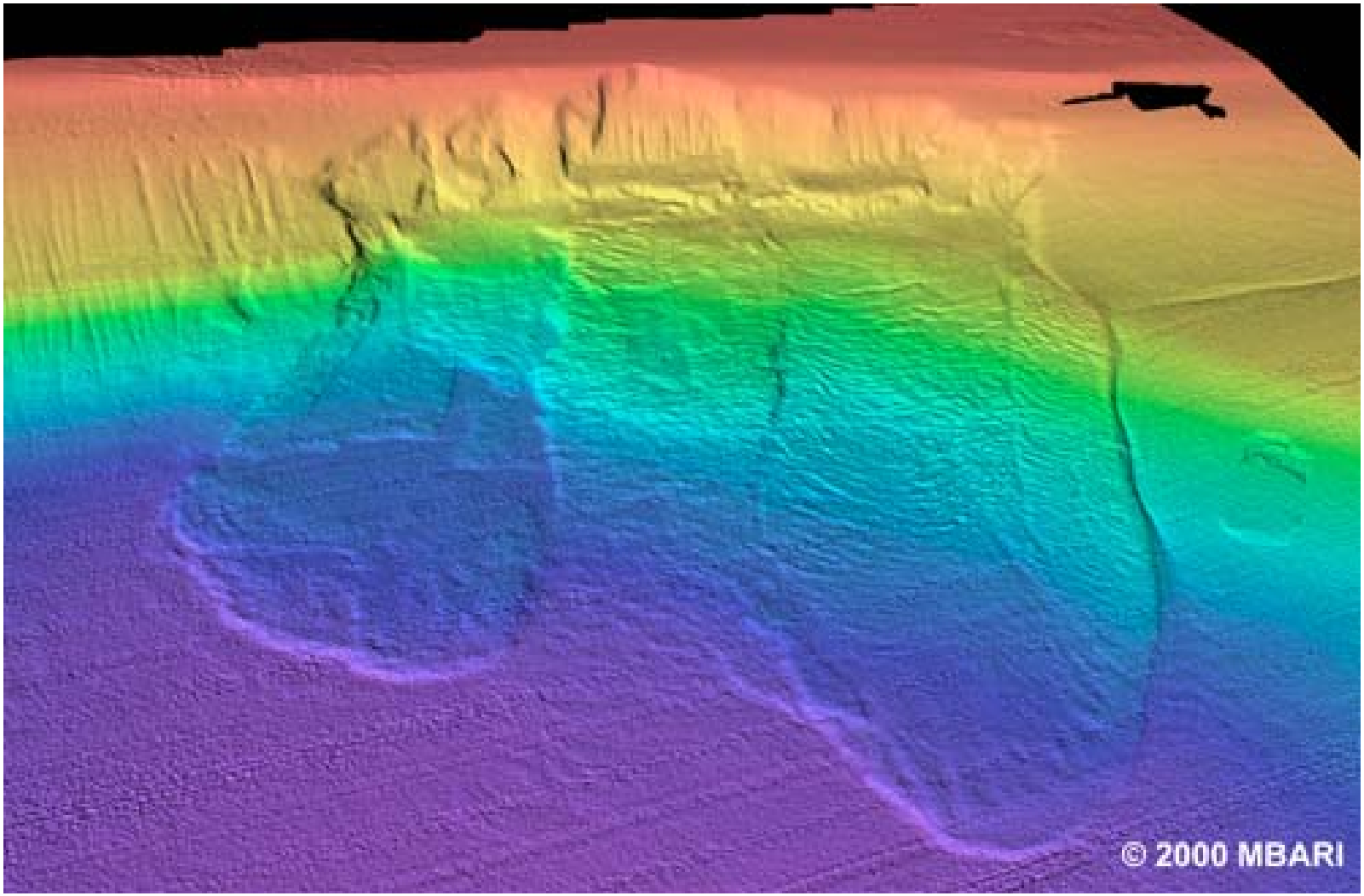

Santa Barbara submarine slide (http://www.mbari.org/)

Motivation

- Formation of topographical features: submarine channels, levees, gullies, sediment waves

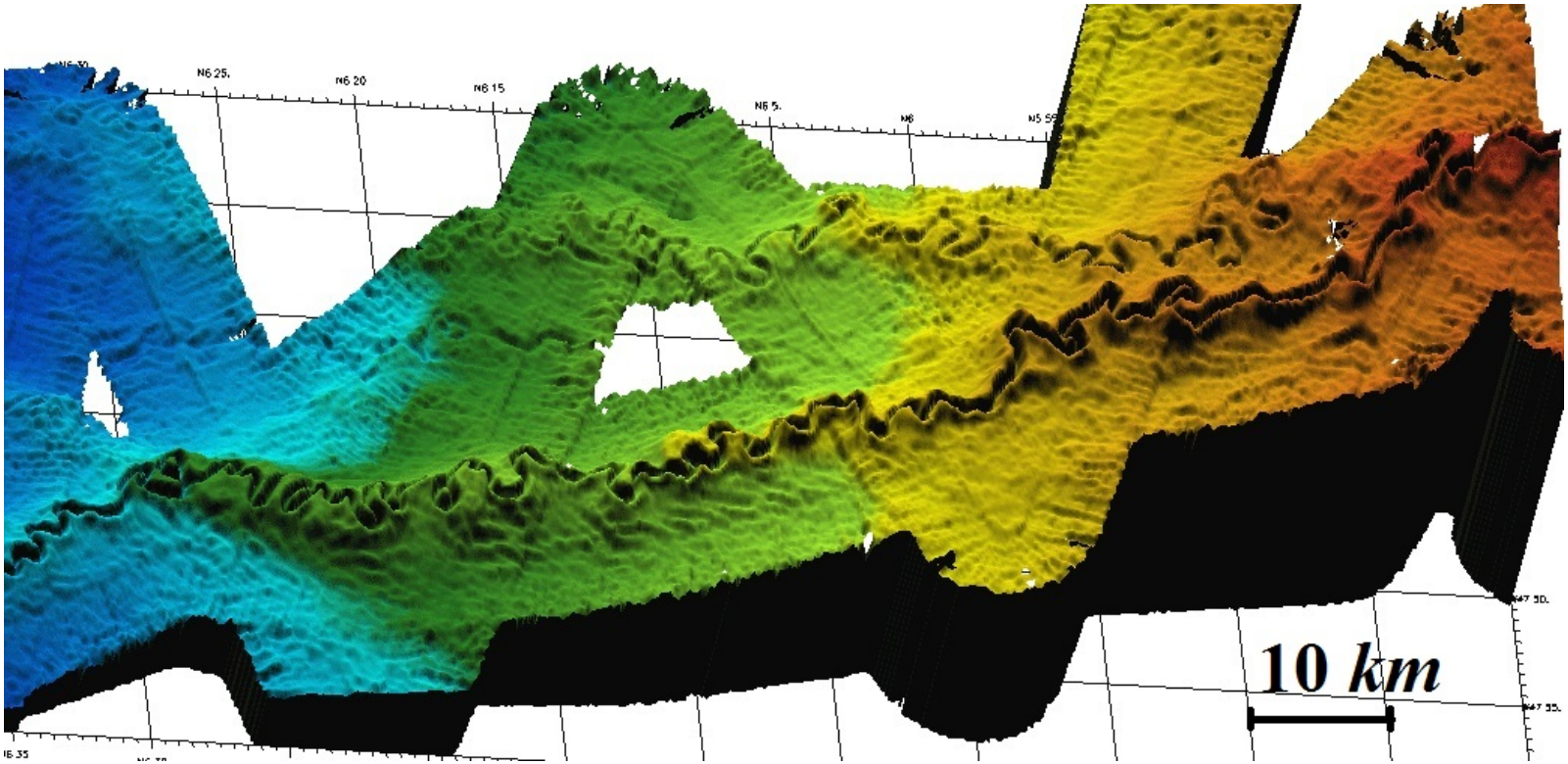

Amazon submarine channel (www.see.leeds.ac.uk/)

Motivation

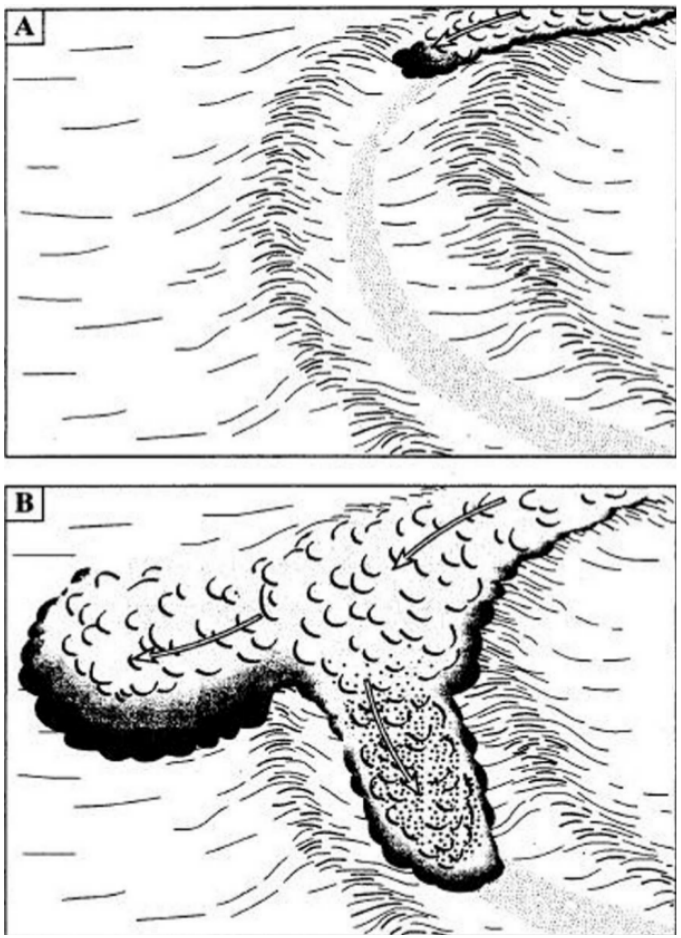

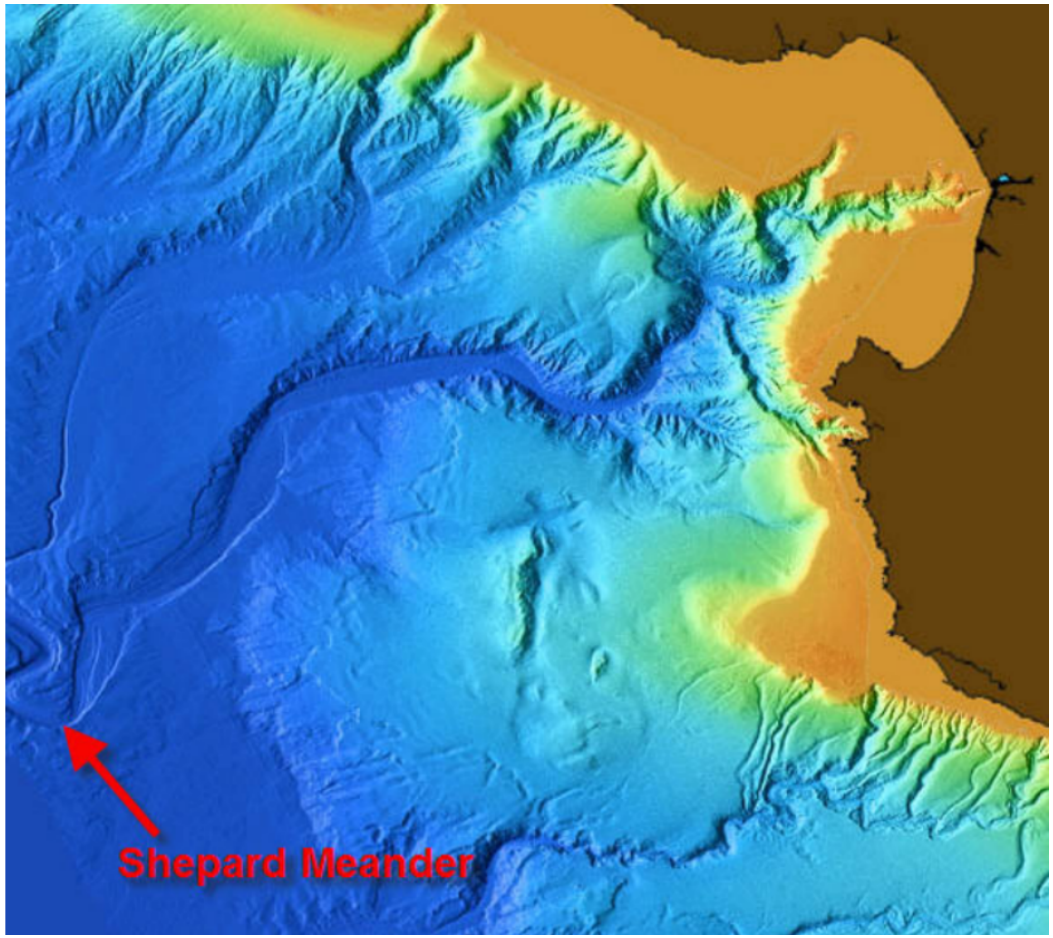

Left: Flow stripping (Peakall *et al.* (2000)) Right: Shepard meander (MBARI 2003, http://www.mbari.org/)

Motivation: Submarine structure design

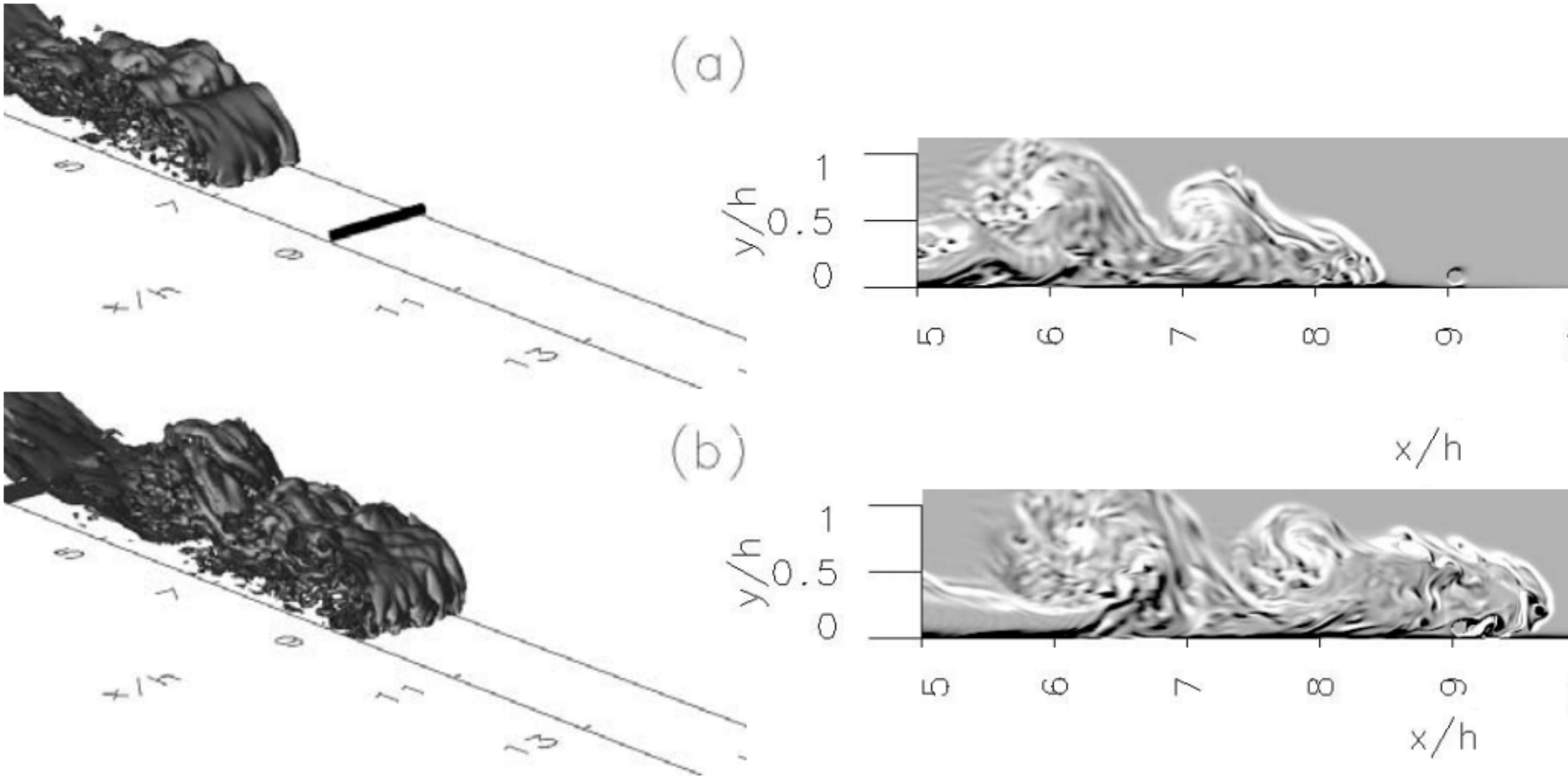

Gravity current interacting with a submarine pipeline (Gonzalez-Juez *et al.* (2010))

Our goals

- Understand various features of turbidity currents
- Influence of complex topography on mixing dynamics, current structure, energy budgets, and deposit profiles
- Our tool: Direct Numerical Simulations (DNS)

Outline

- Modeling approach and assumptions
- Numerical method in TURBINS
- Results and discussion
- Summary

Modeling approach: Basic assumptions

- Dilute suspensions of particles $O(1)\%$ volume fractions
- No particle-particle interactions
- Incompressible flow
- Boussinesq approximations
- No change in bottom bed height as particles settle out
- No erosion and/or bedload transport

Modeling approach: Lock-exchange configuration

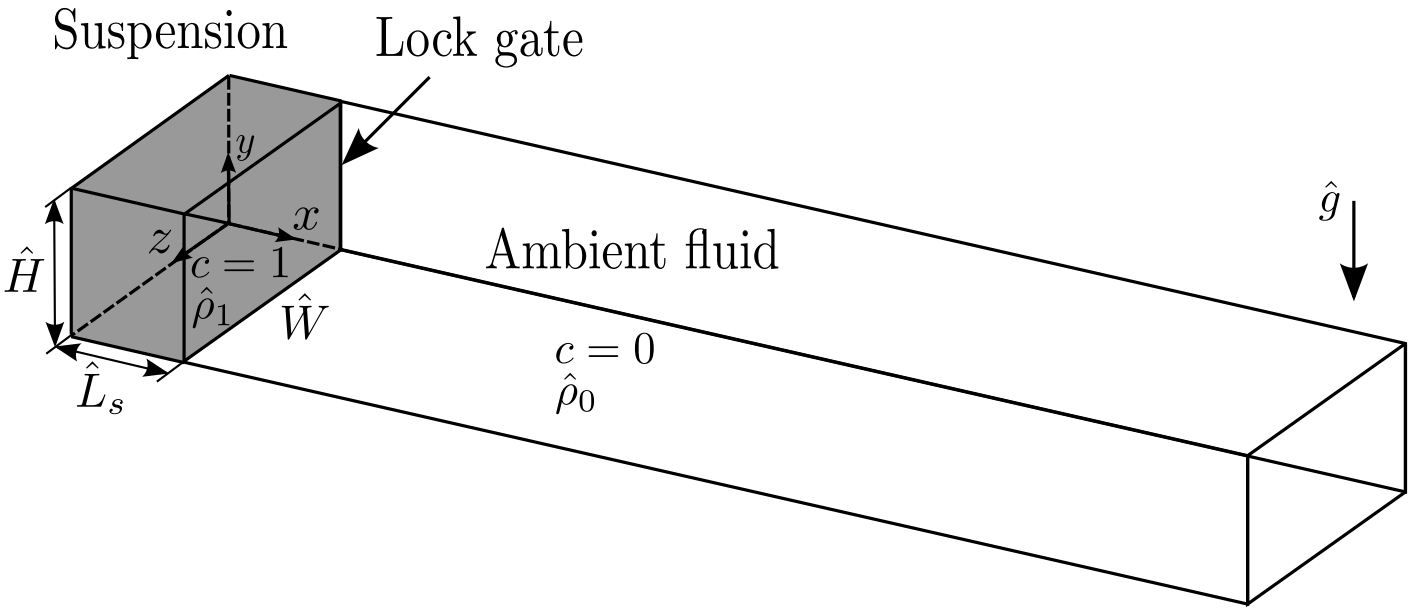

Schematic of the so-called lock-exchange configuration. Lock (gray area), initially, is separated from the ambient fluid by a membrane. Upon release, a turbidity current forms and penetrates along the bottom surface into the ambient fluid.

Modeling approach: Governing equations

- Continuity equation: Incompressible flow

$$\boldsymbol{\nabla} \cdot \mathbf{u} = 0$$

Modeling approach: Governing equations

- Continuity equation: Incompressible flow

$$\boldsymbol{\nabla} \cdot \mathbf{u} = 0$$

- Conservation of momentum: Navier-Stokes equations in Boussinesq approximations

$$\frac{\partial \mathbf{u}}{\partial t} + \mathbf{u} \cdot \boldsymbol{\nabla} \mathbf{u} = -\boldsymbol{\nabla} p + \frac{1}{Re} \nabla^2 \mathbf{u} + \underbrace{c\mathbf{e}^g}_{\text{effective density}}$$

Modeling approach: Governing equations

- Continuity equation: Incompressible flow

$$\boldsymbol{\nabla} \cdot \mathbf{u} = 0$$

- Conservation of momentum: Navier-Stokes equations in Boussinesq approximations

$$\frac{\partial \mathbf{u}}{\partial t} + \mathbf{u} \cdot \boldsymbol{\nabla} \mathbf{u} = -\boldsymbol{\nabla} p + \frac{1}{Re} \nabla^2 \mathbf{u} + \underbrace{c\mathbf{e}^g}_{\text{effective density}}$$

- Small particle size: Neglect inertia

$$\frac{\partial c}{\partial t} + (\mathbf{u} + u_s \mathbf{e}^g) \cdot \boldsymbol{\nabla} c = \frac{1}{ScRe} \nabla^2 c$$

Modeling approach: Important numbers

- Reynolds number

$$Re \equiv \frac{\hat{u}_b \hat{H}/2}{\hat{\nu}}, \quad \text{with} \quad \hat{u}_b = \sqrt{\hat{g}\frac{\hat{\rho}_1 - \hat{\rho}_0}{\hat{\rho}_0}\frac{\hat{H}}{2}}$$

- Schmidt number (no significant influence when $Sc \geq 1$)

$$Sc \equiv \frac{\hat{\nu}}{\hat{\kappa}}$$

- Dimensionless particle settling speed

$$u_s \equiv \frac{\hat{U}_s}{\hat{u}_b}$$

Numerical method: TURBINS

- Viscous terms: Implicit second-order finite difference scheme
- Convective terms: Third-order ENO
- Time integration: Third-order TVD Runge-Kutta method
- To impose a divergence-free velocity field: Fractional projection method
- Complex topography: Immersed boundary method with direct forcing

Numerical method: Parallelism

- Domain decomposition approach using MPI
- Parallel Krylov iterative solvers: PETSc
- Algebraic Multigrid preconditioning for solution of the Poisson equation: BoomerAMG provided by *hypre*

Results: Problem setup

- Two particle sizes with settling velocities: $u_s^c = 0.03$ and $u_s^f = 0.006$
- Mass fractions: coarse particles 50% and 50% of fine particles
- Bottom topography: Gaussian bumps

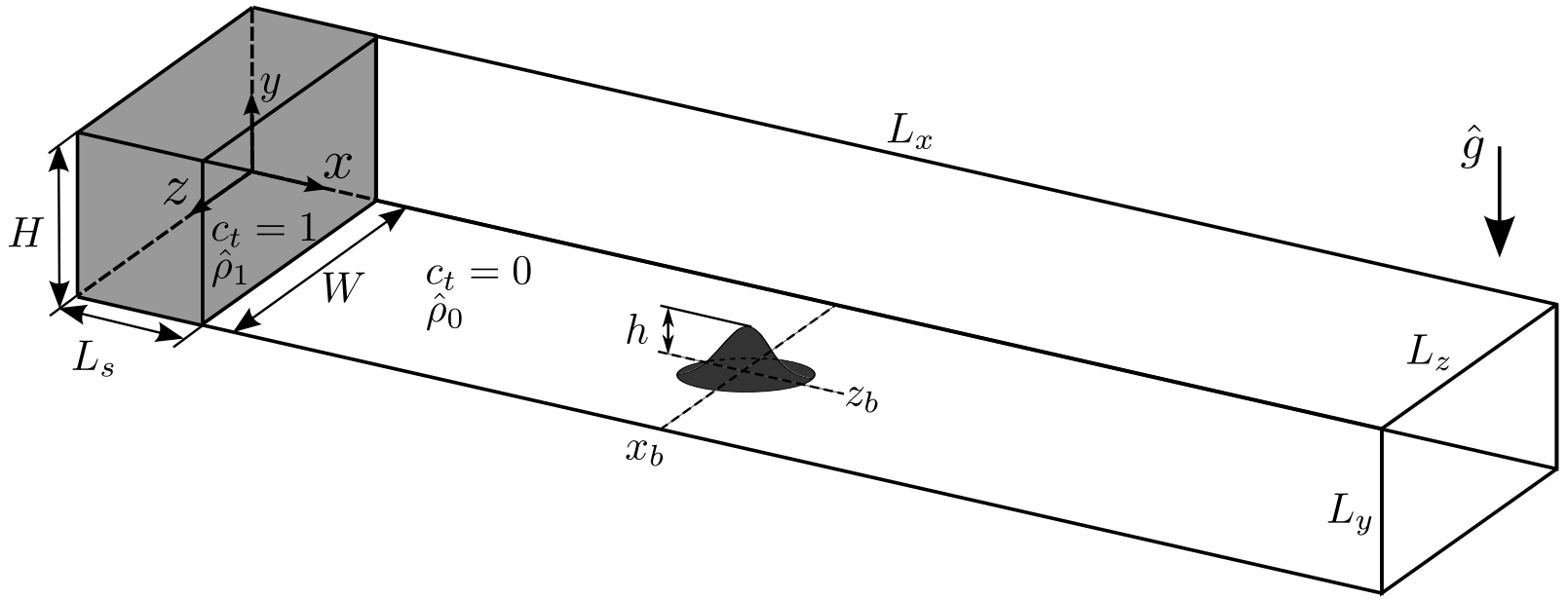

Results: Problem setup

Sim.	h	(x_b, z_b)	Re	(L_x, L_y, L_z)
FL	0.0	N/A	2000	(38,2,3)
B1	0.25	(5.5,1.5)	2000	(38,2,3)
B2	0.5	(5.5,1.5)	2000	(38,2,3)

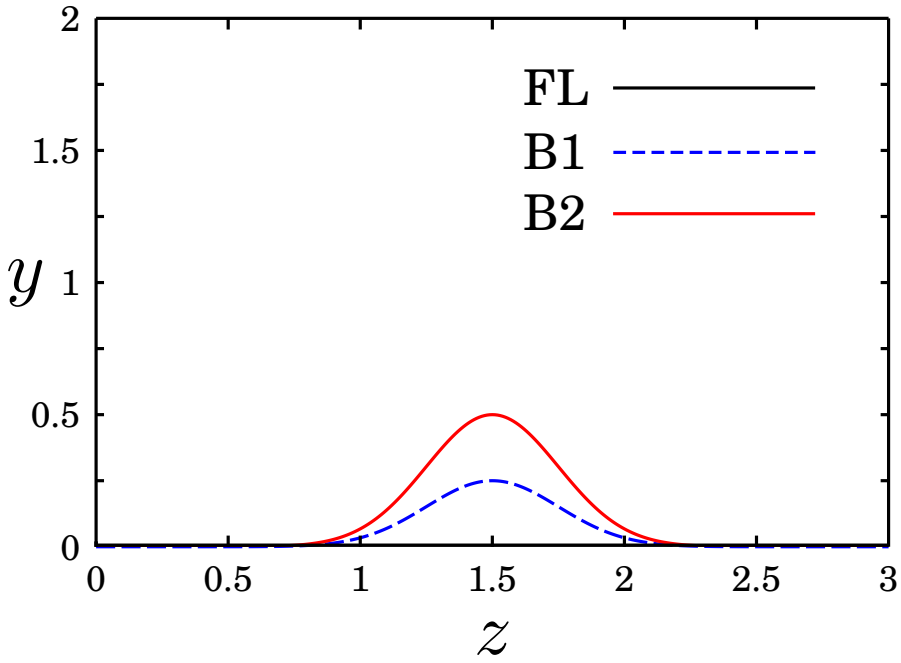

Results: Flow evolution

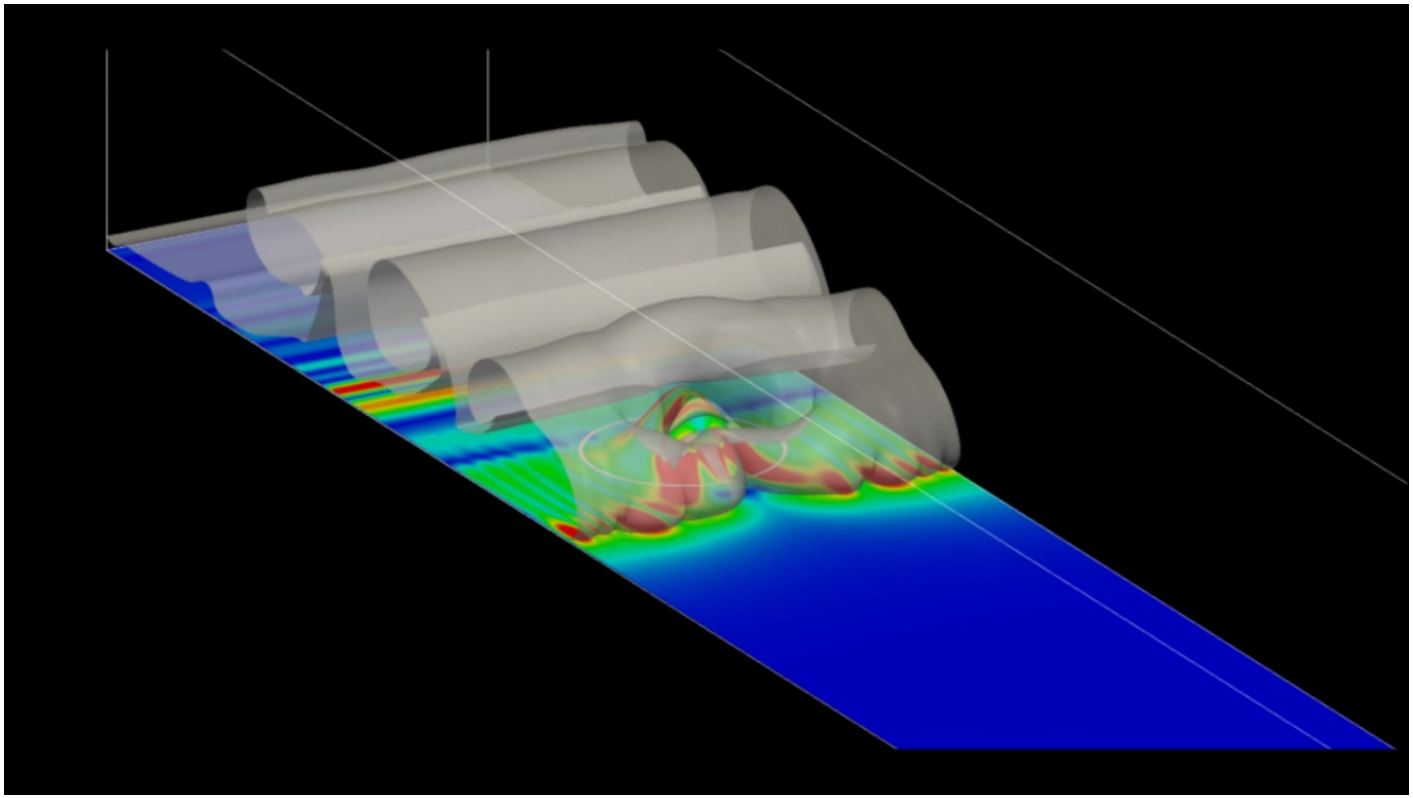

Results: Frontal structure

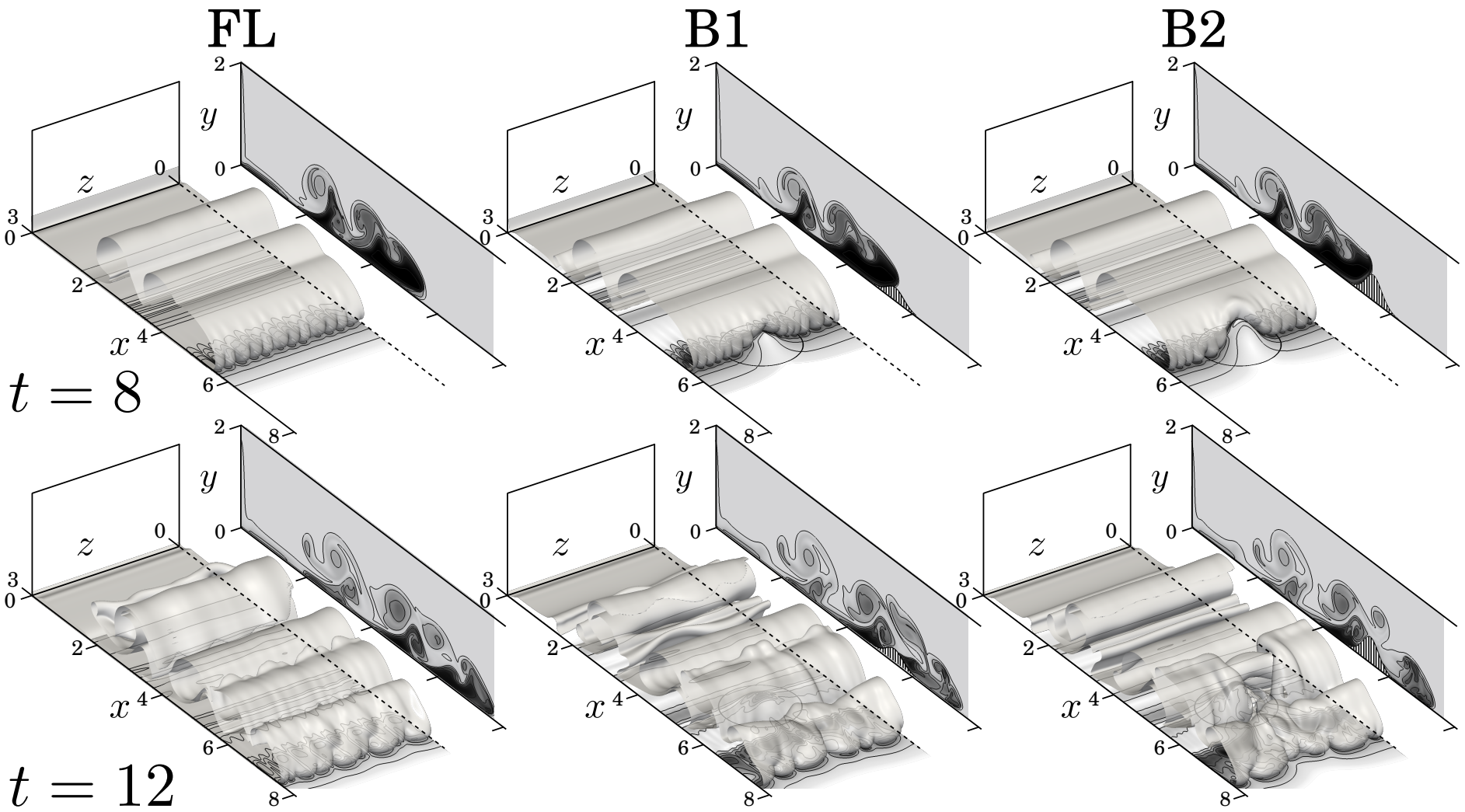

Results: Frontal structure

Current front is bi-sected in case B2.

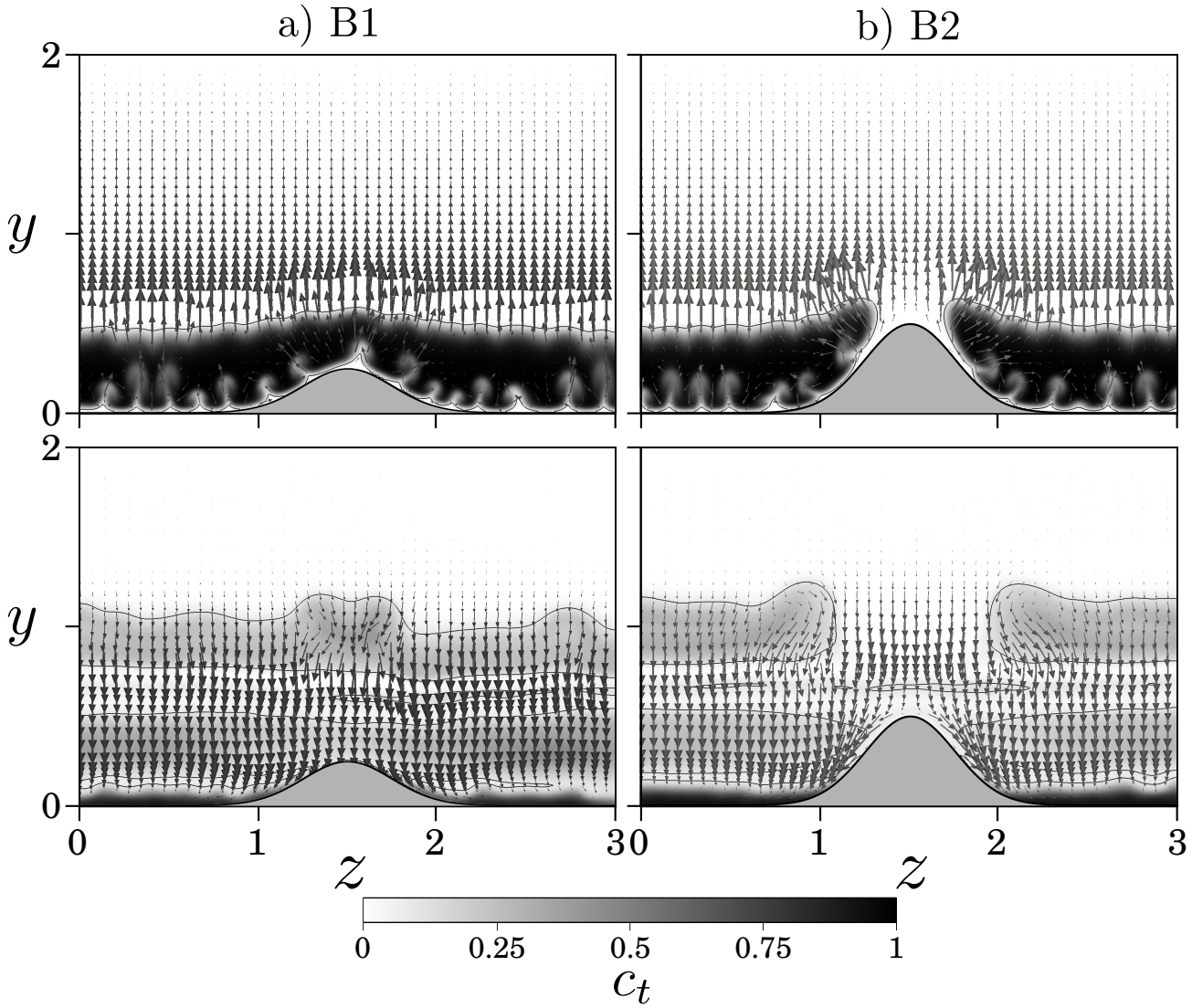

Results: Vortical structures

Vortical structures are identified by Q-criterion

$$
\begin{aligned}
Q &= \frac{1}{2}(\Omega_{ij}\Omega_{ij} - S_{ij}S_{ij})\,, \\
\Omega_{ij} &= \frac{1}{2}(\frac{\partial u_i}{\partial x_j} - \frac{\partial u_j}{\partial x_i})\,, \\
S_{ij} &= \frac{1}{2}(\frac{\partial u_i}{\partial x_j} + \frac{\partial u_j}{\partial x_i})\,.
\end{aligned}
$$

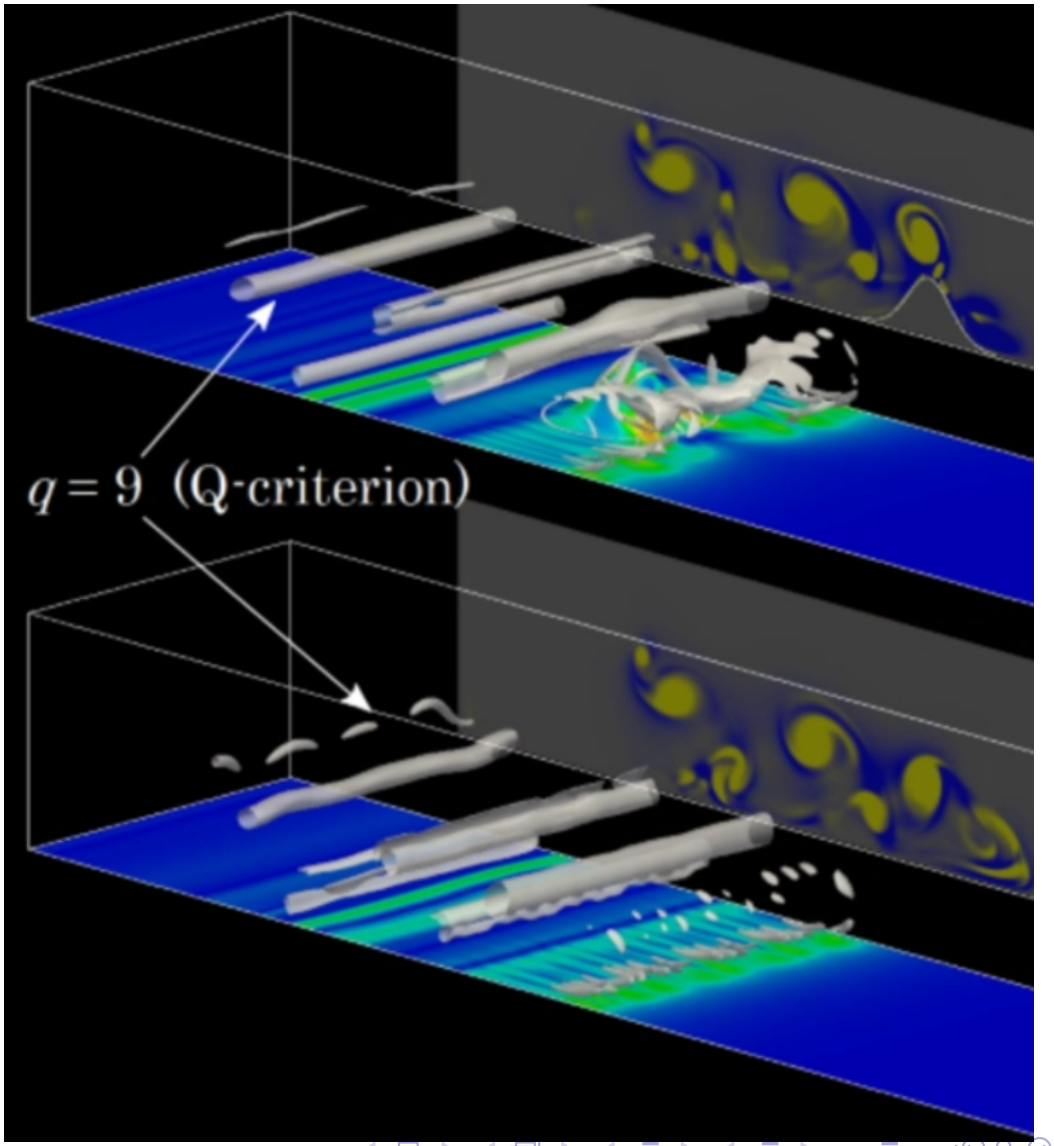

Results: Vortical structures

Production of strong vortices in the shear layer in case B2.

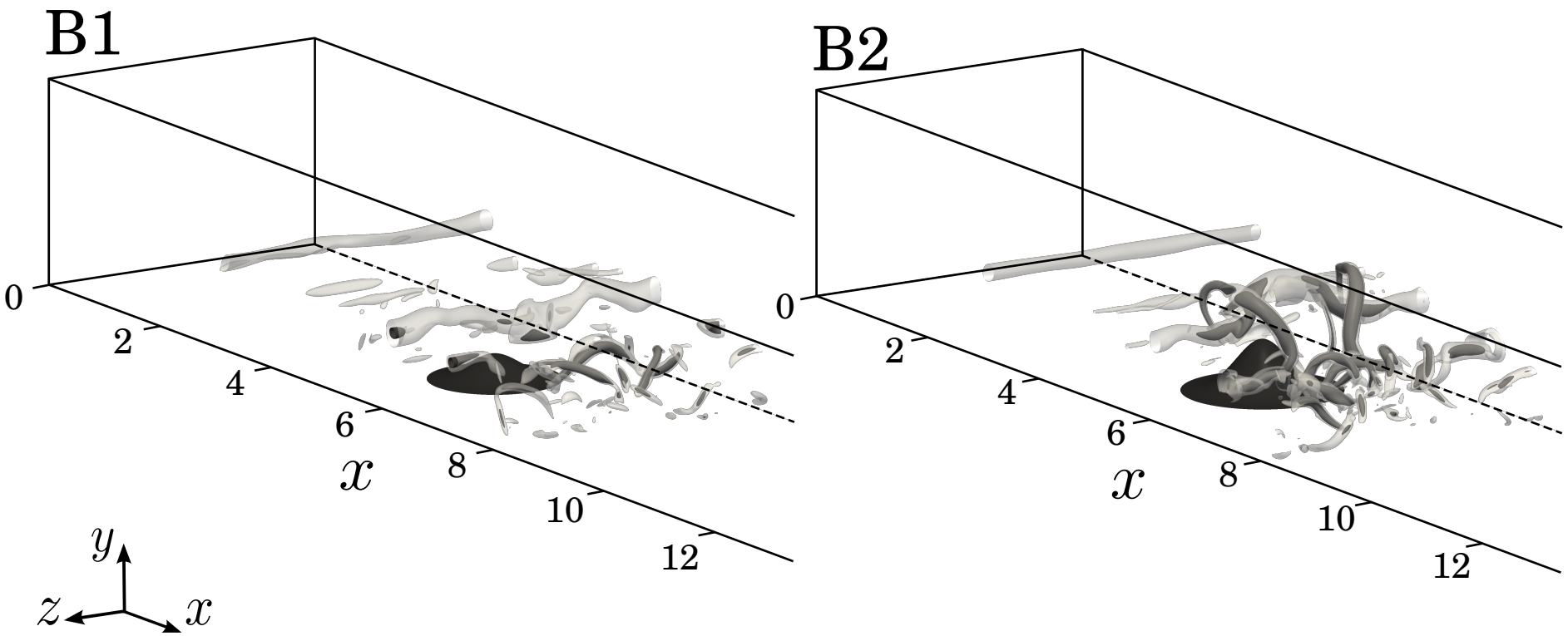

Results: Vortical structures

Production of strong vortices in the shear layer in case B2.

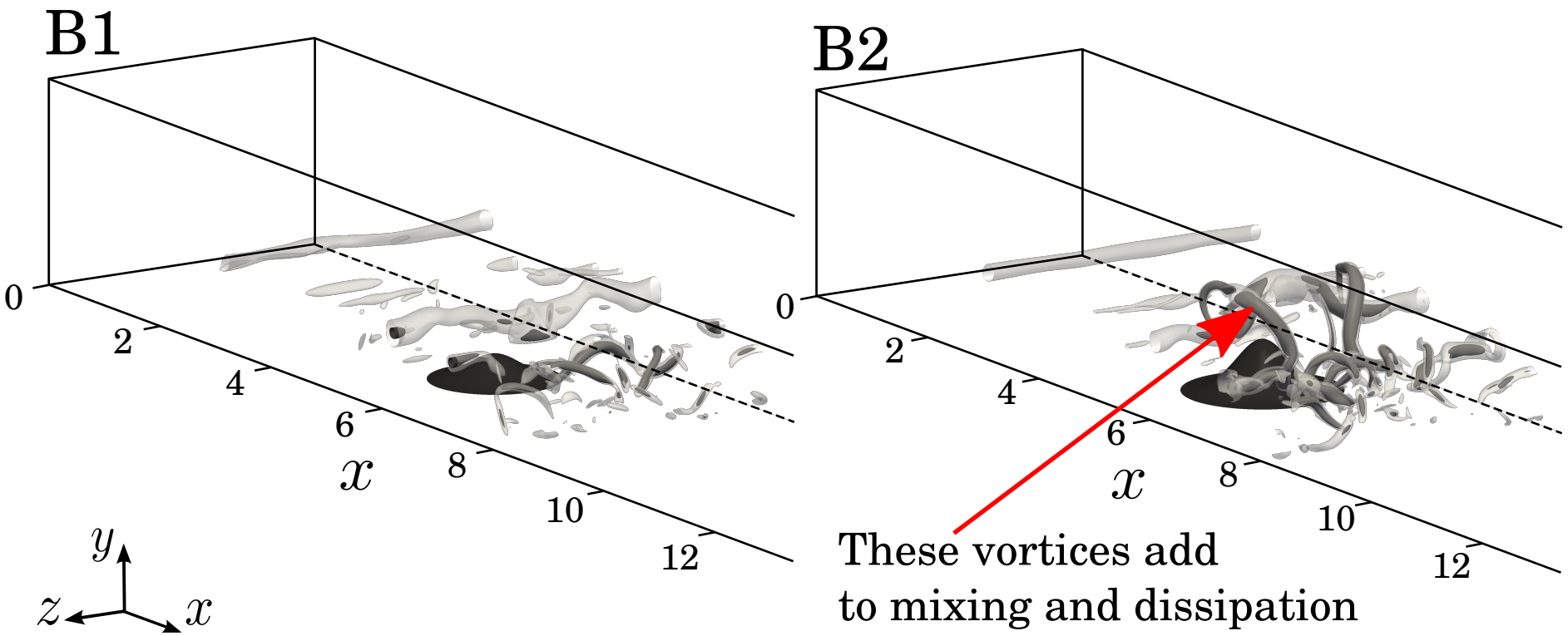

Results: Vortical structures

Generation of the horse-shoe vortex in case B2

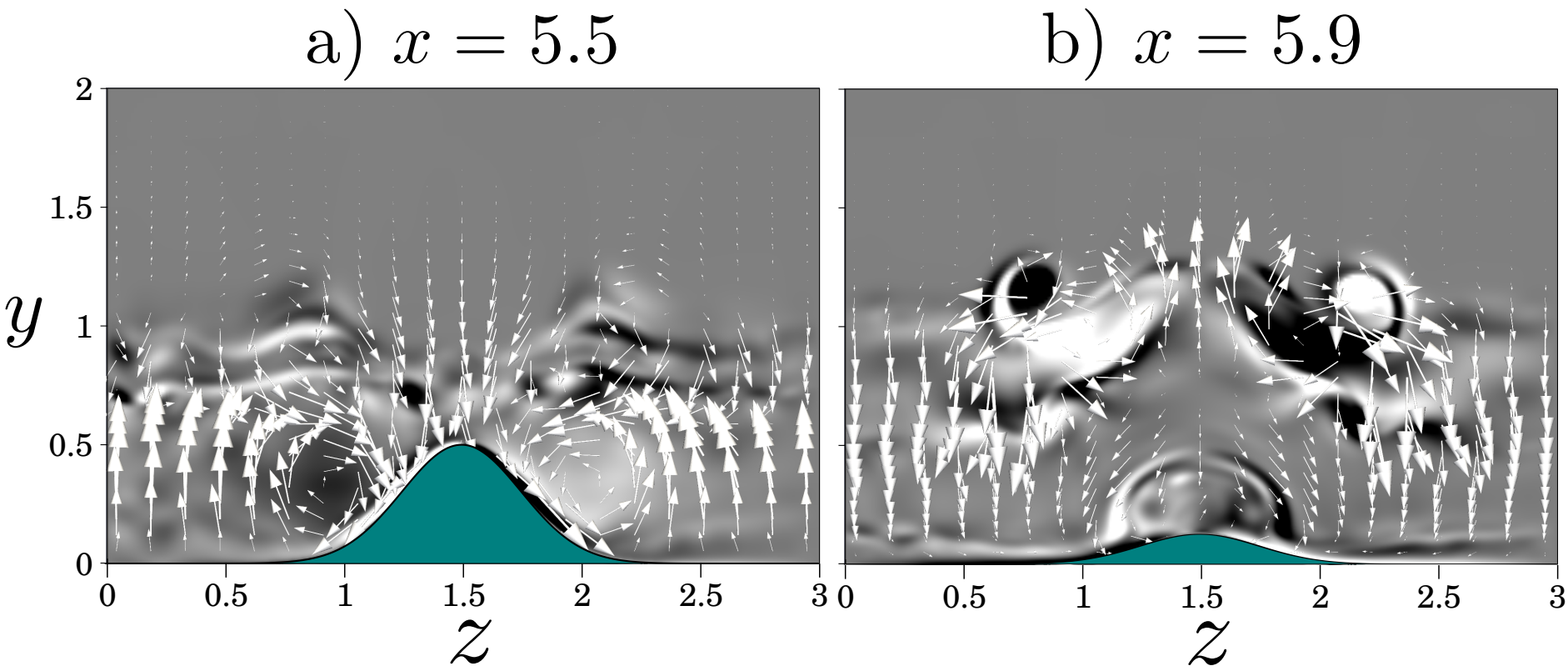

Results: Vortical structures

Generation of the horse-shoe vortex in case B2

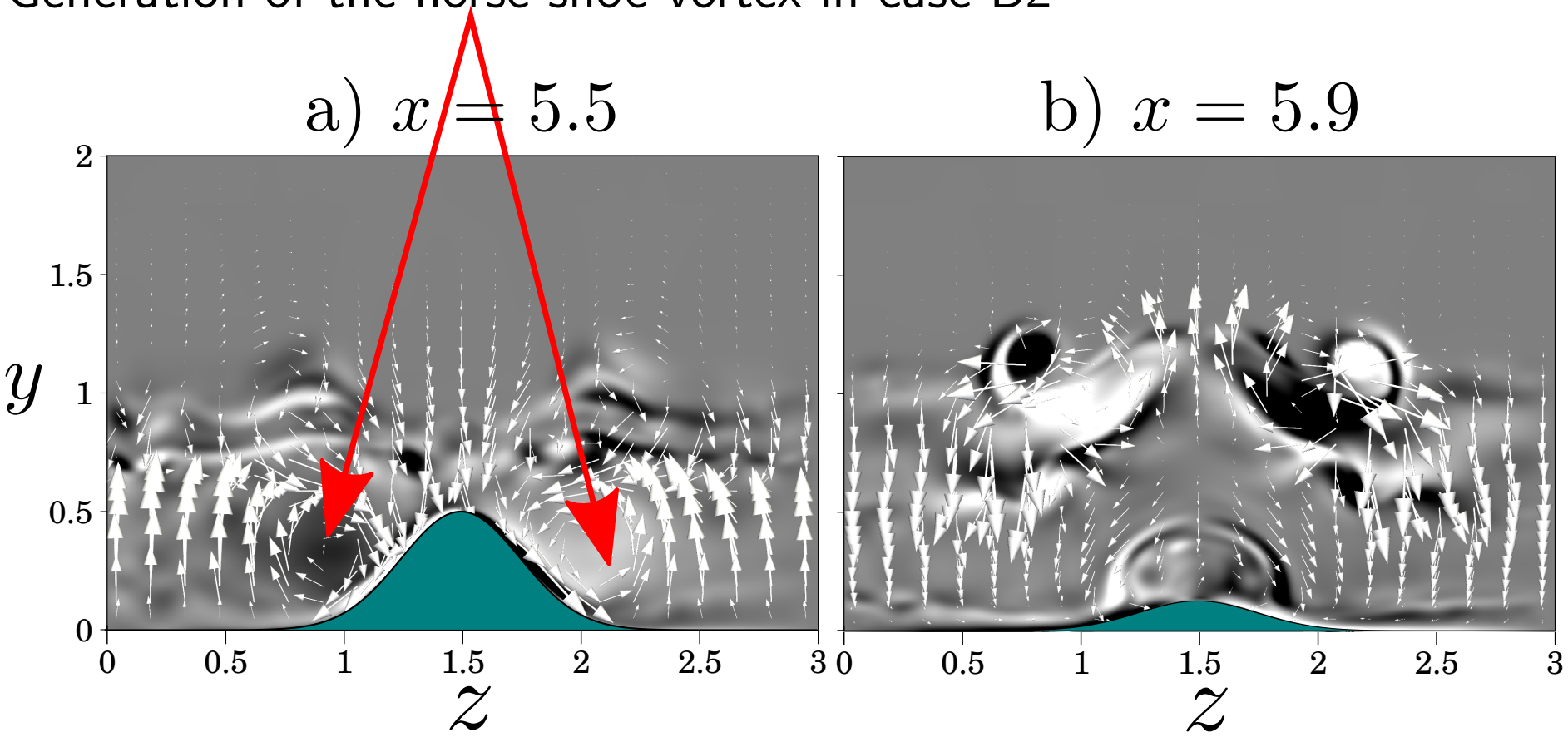

Results: Influence on wall shear stress

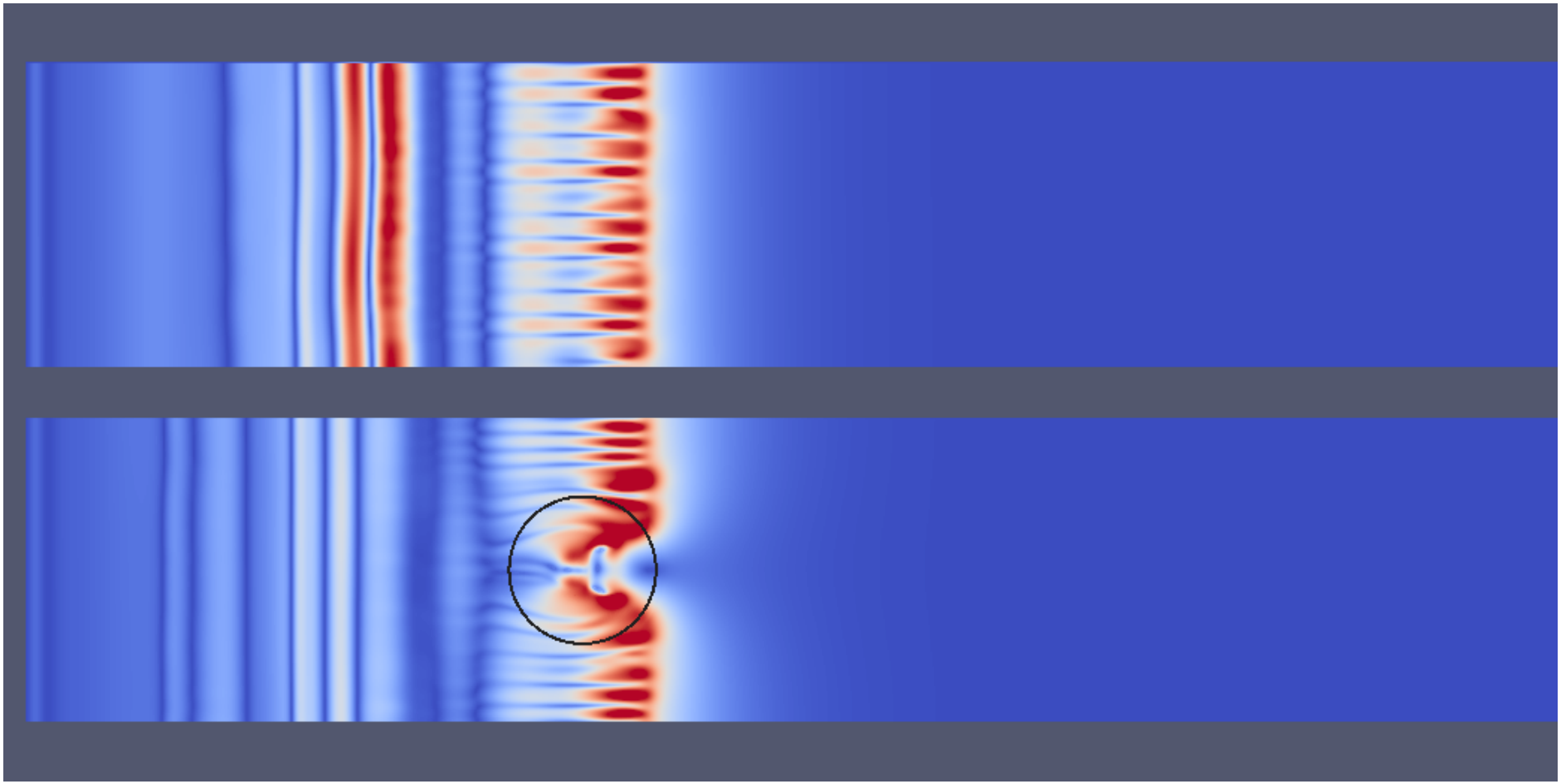

Results: Front location and suspended mass

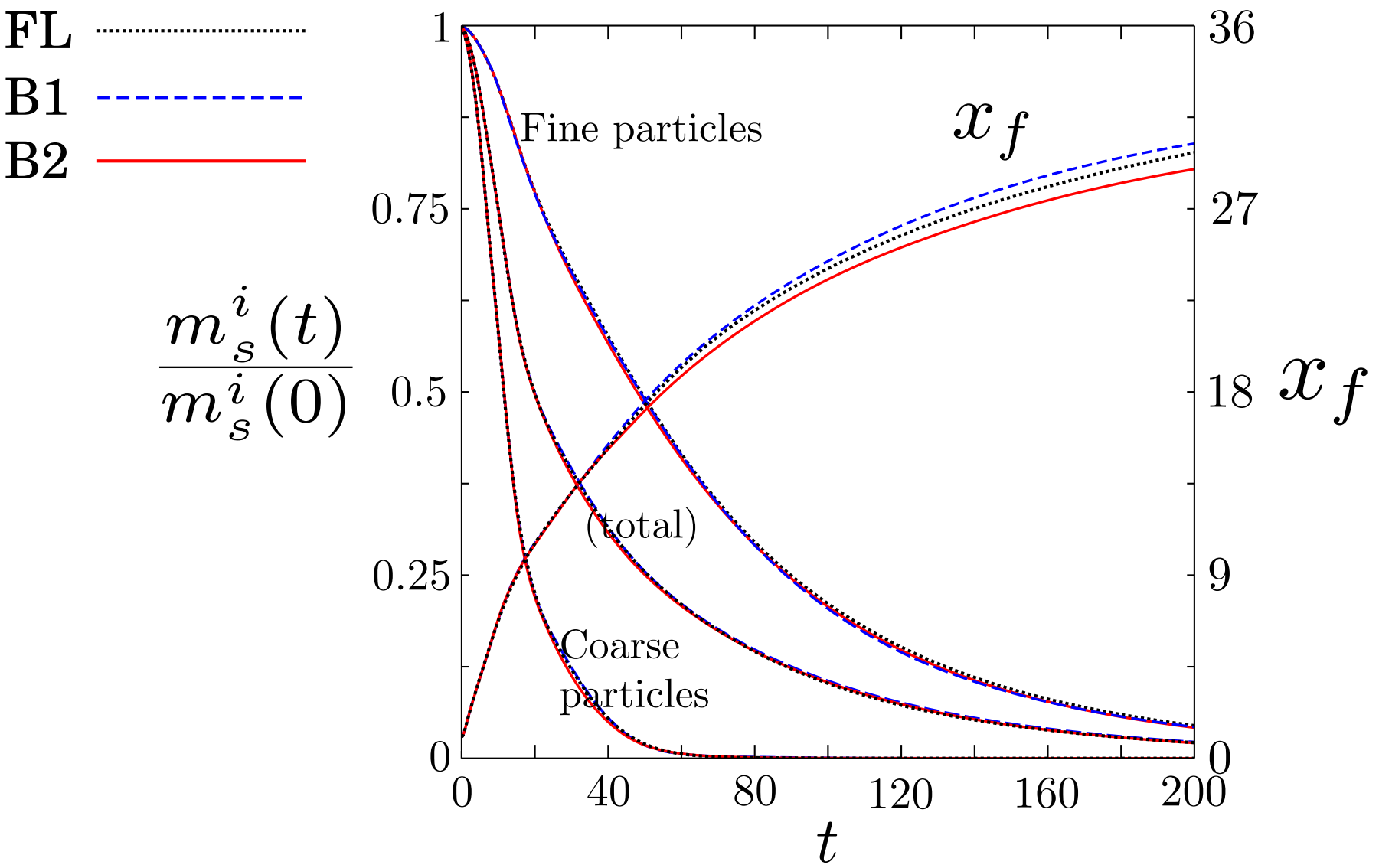

Results: Front location?

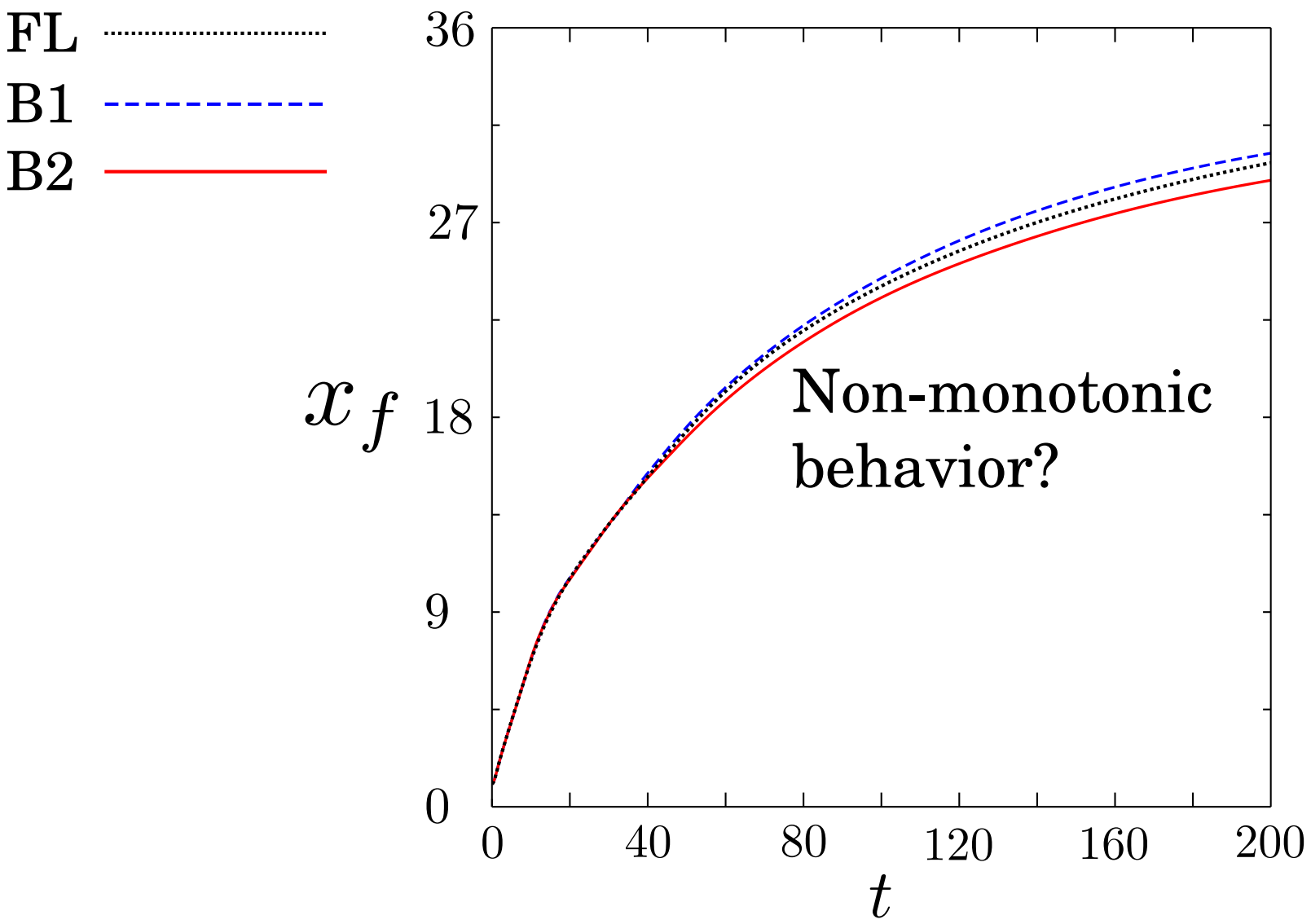

Results: Let's look at the energy components

- Energy conservation equation over the entire volume

$$E_k(t) + E_p(t) + [E_d(t) + E_s(t) + E_l(t)] = \text{const.}$$

Results: Let's look at the energy components

- Energy conservation equation over the entire volume

$$E_k(t) + E_p(t) + [E_d(t) + E_s(t) + E_l(t)] = \text{const.}$$

- Kinetic and potential energies

$$\begin{aligned} E_k(t) &= \frac{1}{2}\int_V \mathbf{u}\cdot\mathbf{u}dV\,, \\ E_p(t) &= \int_V c_t(y - y_{\text{ref}})dV\,. \end{aligned}$$

Results: Let's look at the energy components

- Energy-loss components: Viscous dissipation E_d, Stokes dissipation E_s, and particles leaving the domain E_l

$$\begin{aligned}
\frac{dE_d(t)}{dt} &= \int_V \frac{2}{Re} S_{ij} S_{ij} dV \ , \\
\frac{dE_s(t)}{dt} &= \sum_{i=1}^{2} \left(\int_V u_s^i c_i dV \right) \ , \\
\frac{dE_l(t)}{dt} &= \sum_{i=1}^{2} \left(- \int_A y_\Gamma u_s^i c_w^i \mathbf{e}^g \cdot \mathbf{n} dA \right) \ .
\end{aligned}$$

Results: Let's look at the energy components

Upon arrival of the current at the bump location, viscous dissipation (E_d) in case B2 is further enhanced.

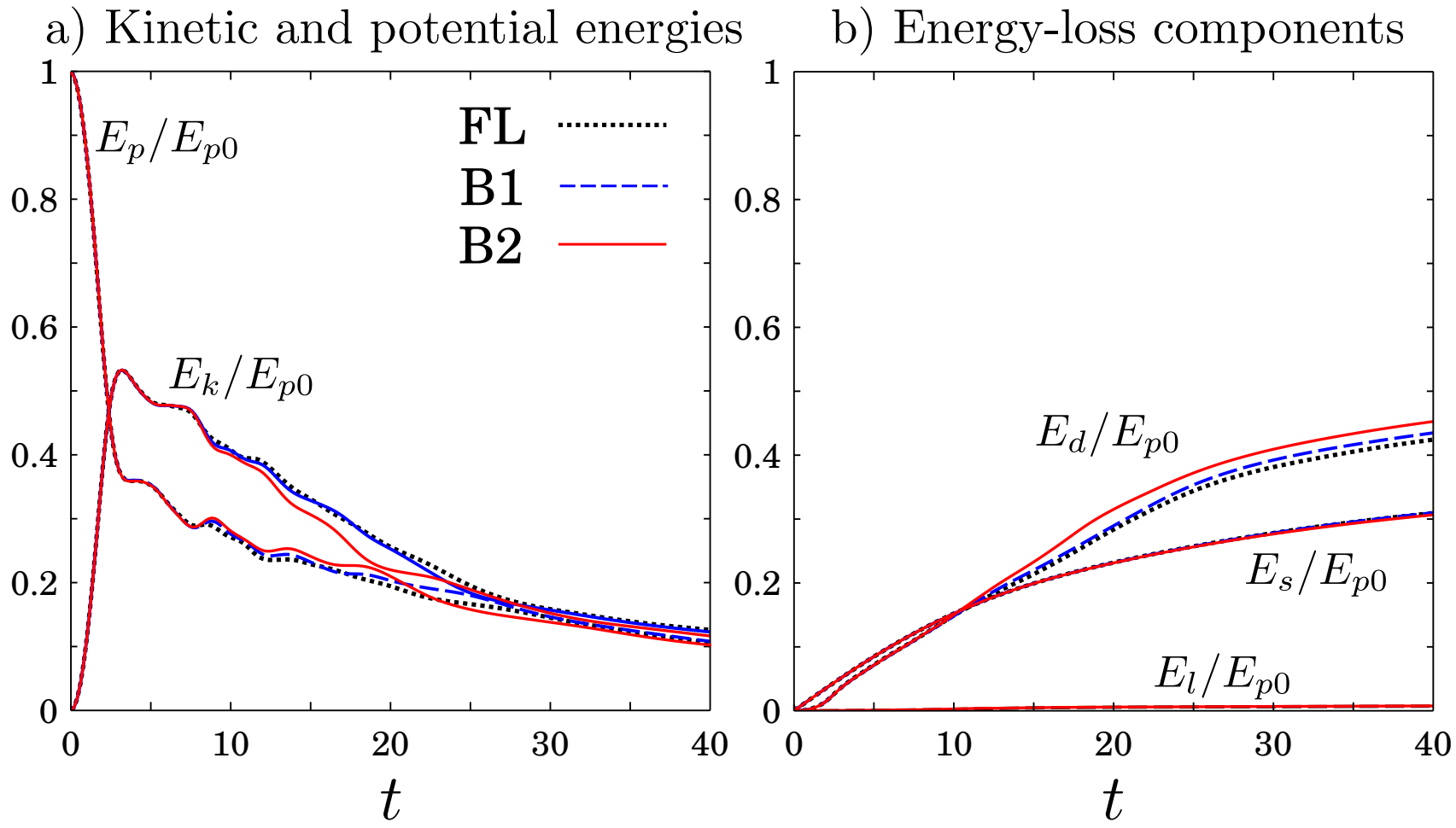

Results: Let's look at the energy components

Upon arrival of the current at the bump location, viscous dissipation (E_d) in case B2 is further enhanced.

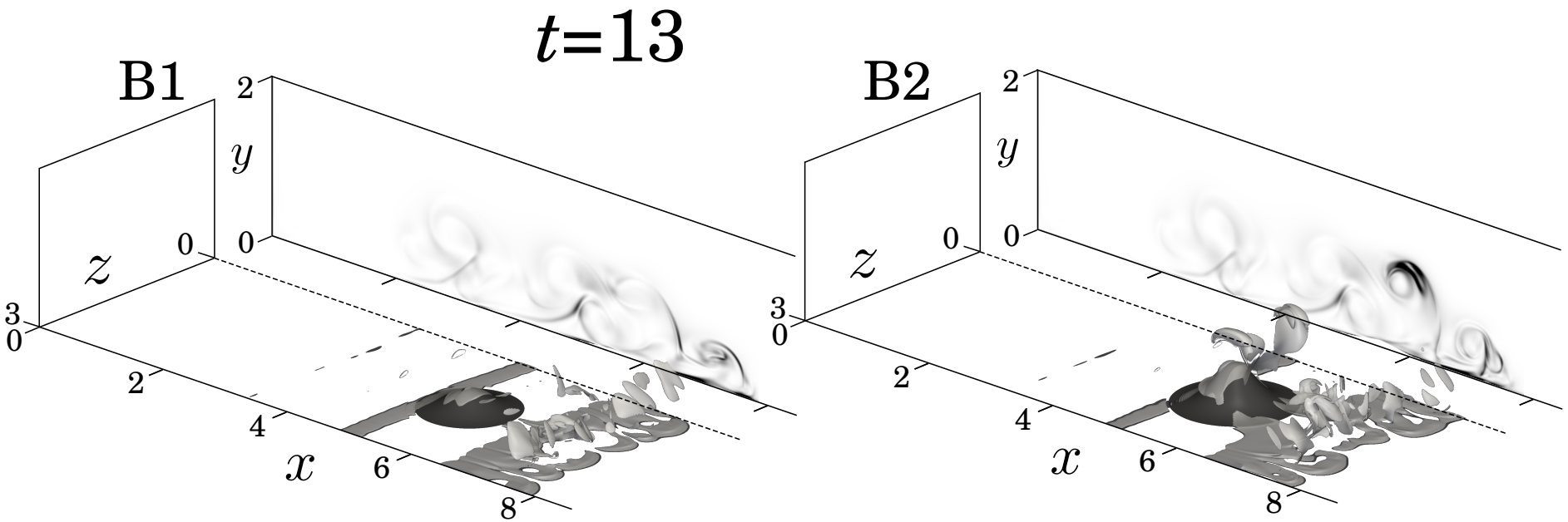

Results: Front velocity and current height

Current thickens: Front velocity increases

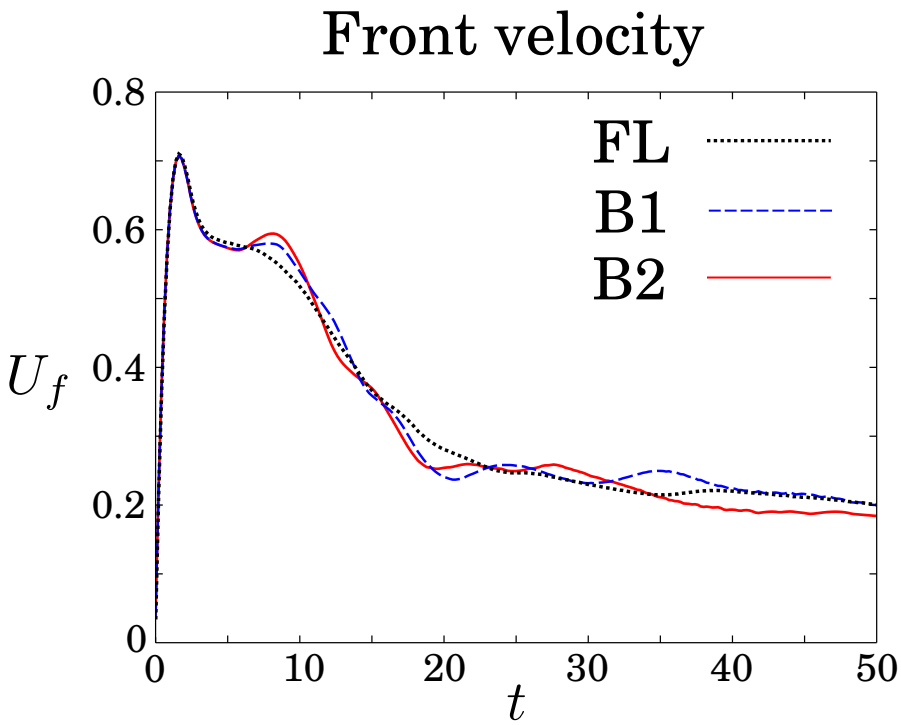

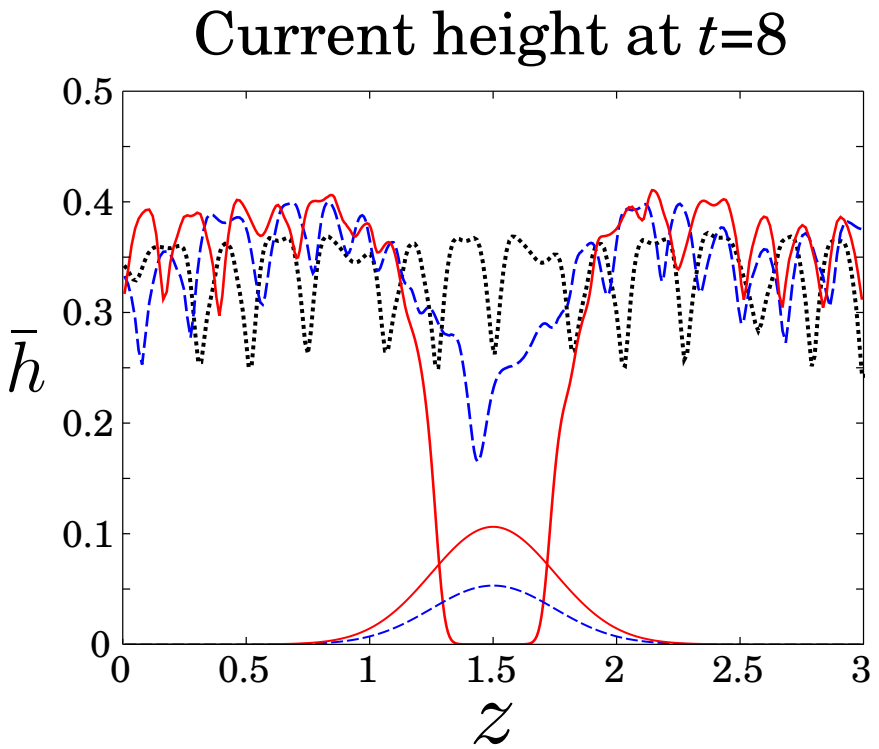

Results: Discussion

With the increase in bump height, there are two competing effects:

- Enhancement in dissipation loss due to generation of vortical structures
- Increase in front velocity due to increase in the current height

When compared to a flat bottom surface: Existence of a critical bump height which indicates the current traveling faster or slower than the flat bottom case.

Results: Does the current travel "over" or "around" the bump?

Is there any simplified model to predict this?

- Set the particle settling velocity to zero.
- Vary the bump height: h_b =0.25, 0.5, 0.75, 1, and 1.25.

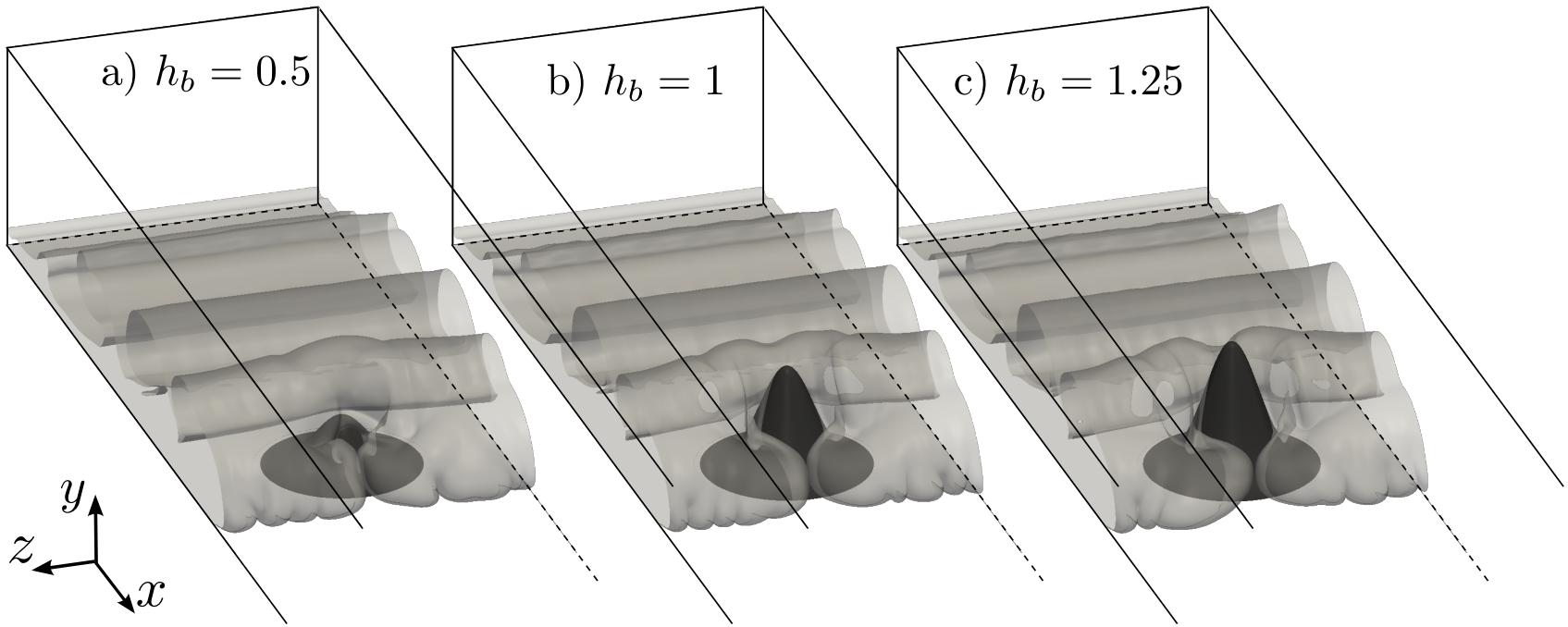

Results: Does the current travel "over" or "around" the bump?

Is there any simplified model to predict this?
Snyder et al (1979) and Snyder et al (1985):

- The lowest section of the current surpasses the obstacle if

$$\frac{\hat{U}_\infty^2}{\hat{g}\hat{h}_c\Delta\hat{\rho}/\hat{\rho}_0} > 2(\frac{\hat{h}_b}{\hat{h}_c} - 1)$$

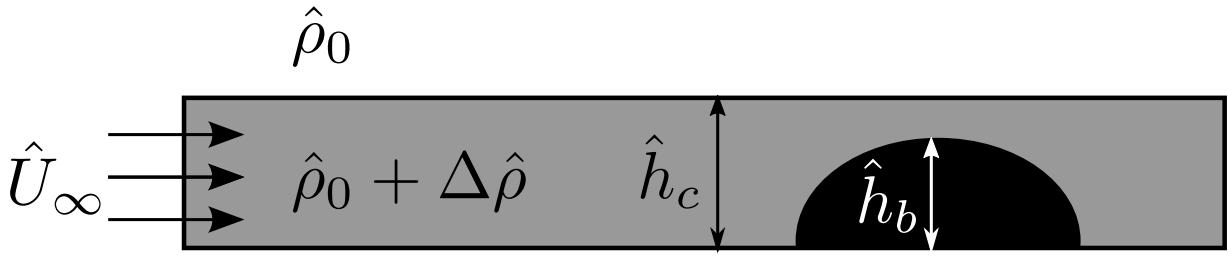

Results: Does the current travel "over" or "around" the bump?

Critical bump height:

- Current upstream of the obstacle: $U_\infty \approx 0.7$ and $h_c \approx 0.7$

$$h_b|_{\text{critical}} \approx 0.9$$

Results: Fluid pathlines

Release four seed passive-markers upstream of the bump to track the fluid parcels belonging to the gravity current (movie)

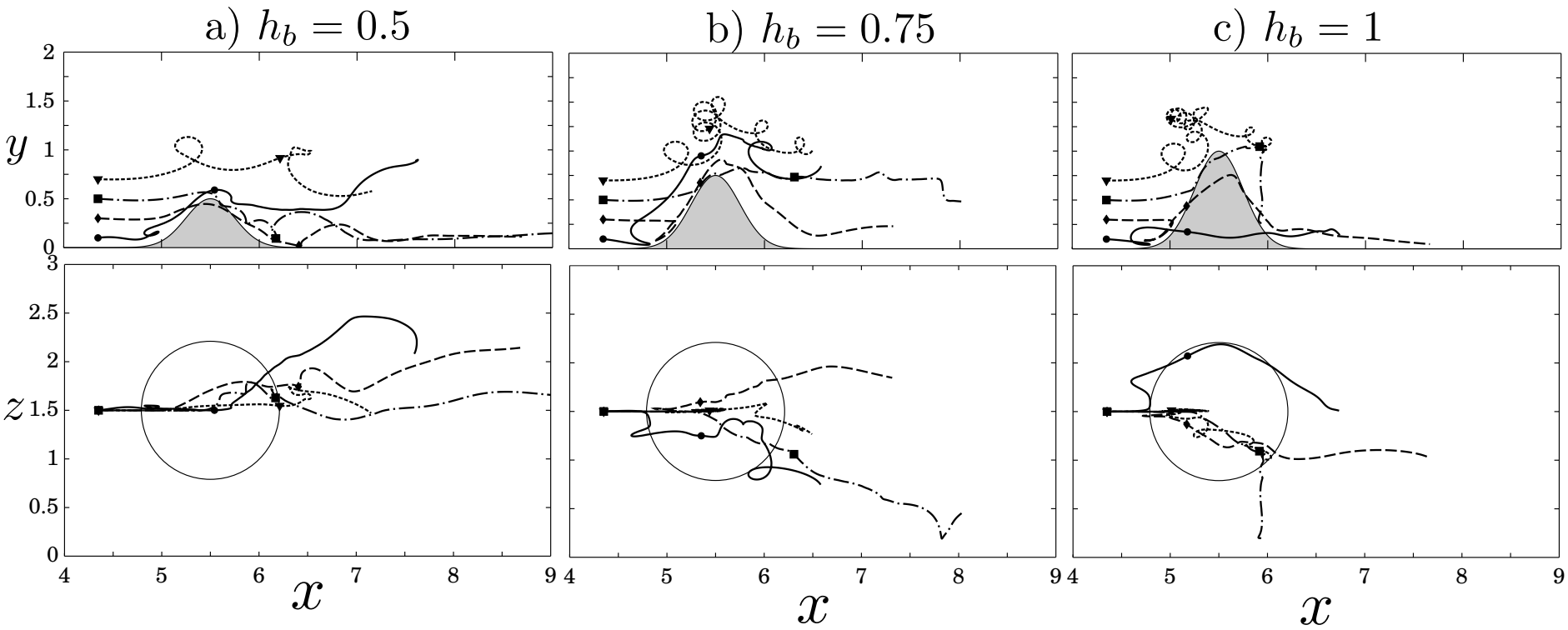

Results: Mixing dynamics

- Lock-fluid (interstitial fluid) is tracked via a concentration field $c_3(x, y, z, t)$.
- c_3 is advected along the fluid velocity $\mathbf{u}$
- Integral quantity Φ^θ is defined to quantify mixing of the ambient and lock fluid

$$\Phi^\theta = \frac{1}{L_s \times H \times W} \int_V G(c_3; c_\theta) dV \qquad \text{with}$$

$$G(c_3; c_\theta) = \begin{cases} 1 & \text{if } \; c_3 \geq c_\theta \,, \\ 0 & \text{if } \; c_3 < c_\theta \,. \end{cases}$$

Results: Influence on mixing

Mixing identified with entrainment of ambient fluid into lock-fluid

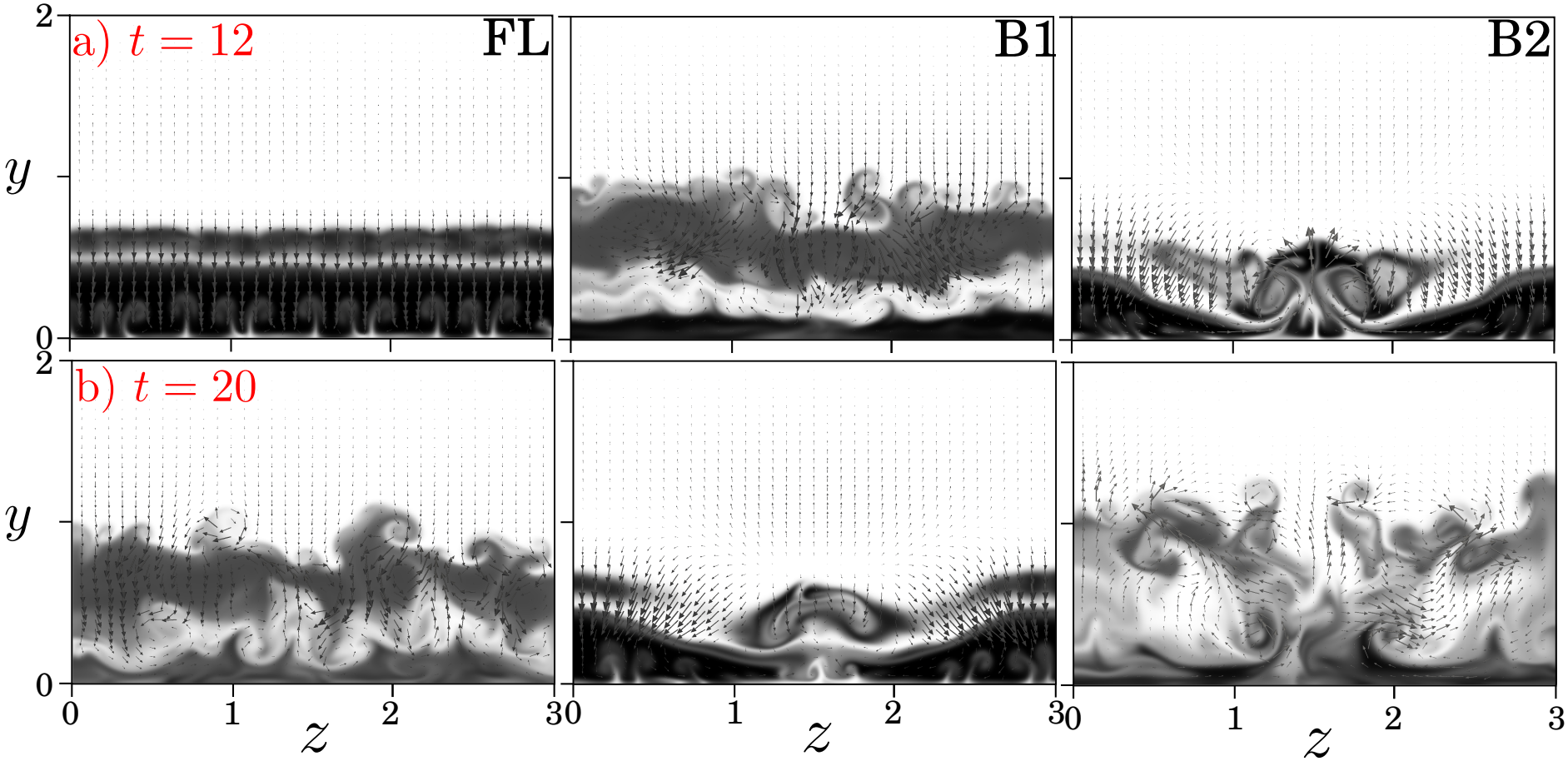

Results: Influence on mixing

Φ: Entrainment of ambient fluid into lock fluid

c_θ: Mixing concentration threshold

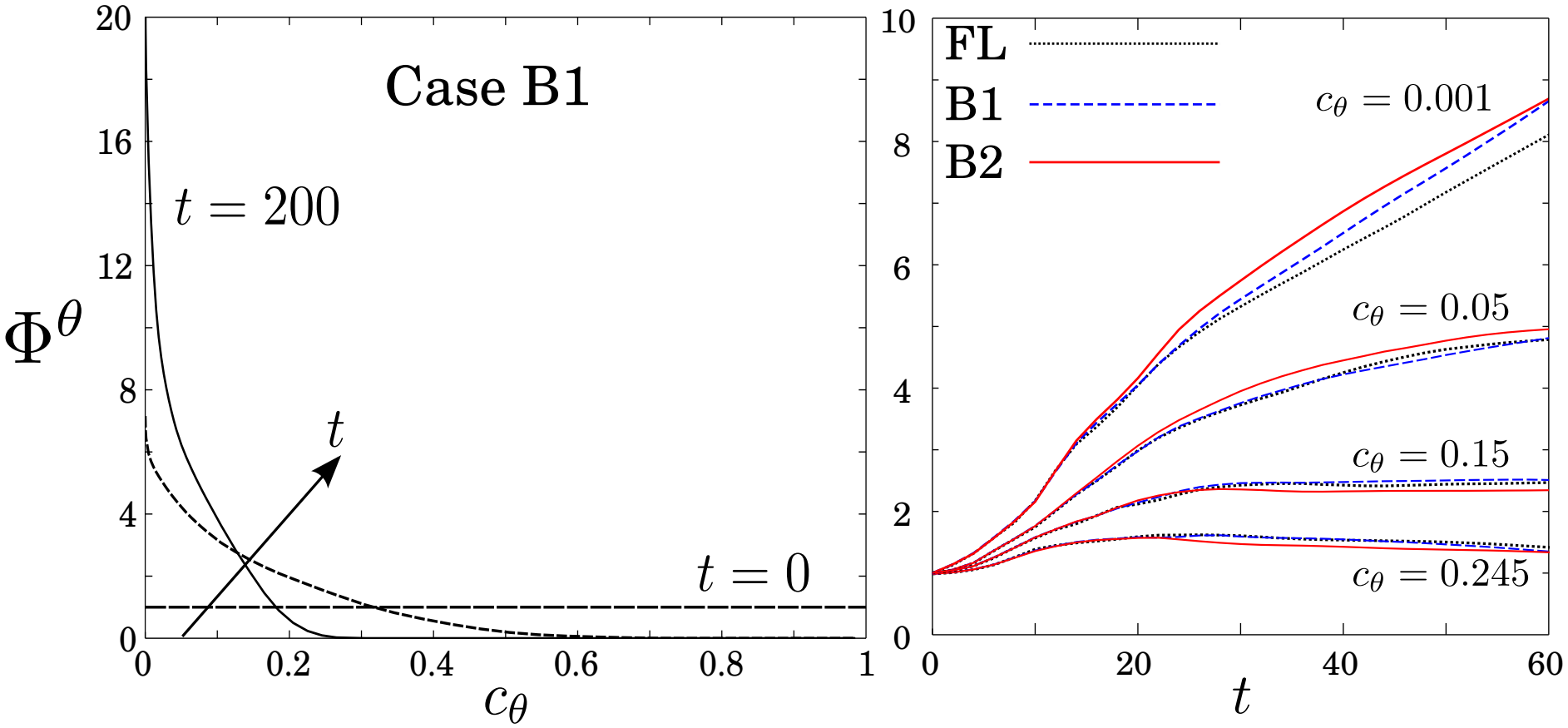

Results: Gravity vs turbidity current

Run case B2 with zero settling velocity (B2-GC)
Mixing is more pronounced in case with particles.

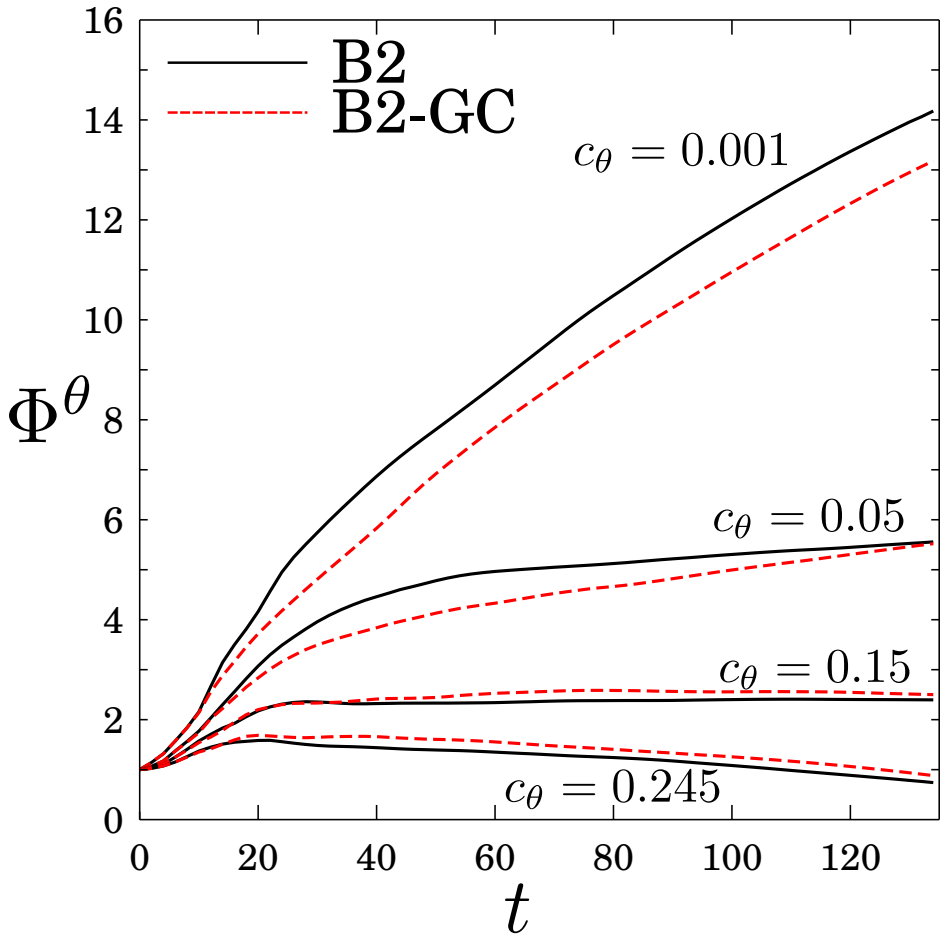

Results: Gravity vs turbidity current

Case B2-GC (gravity current) is faster than B2 (particles)?

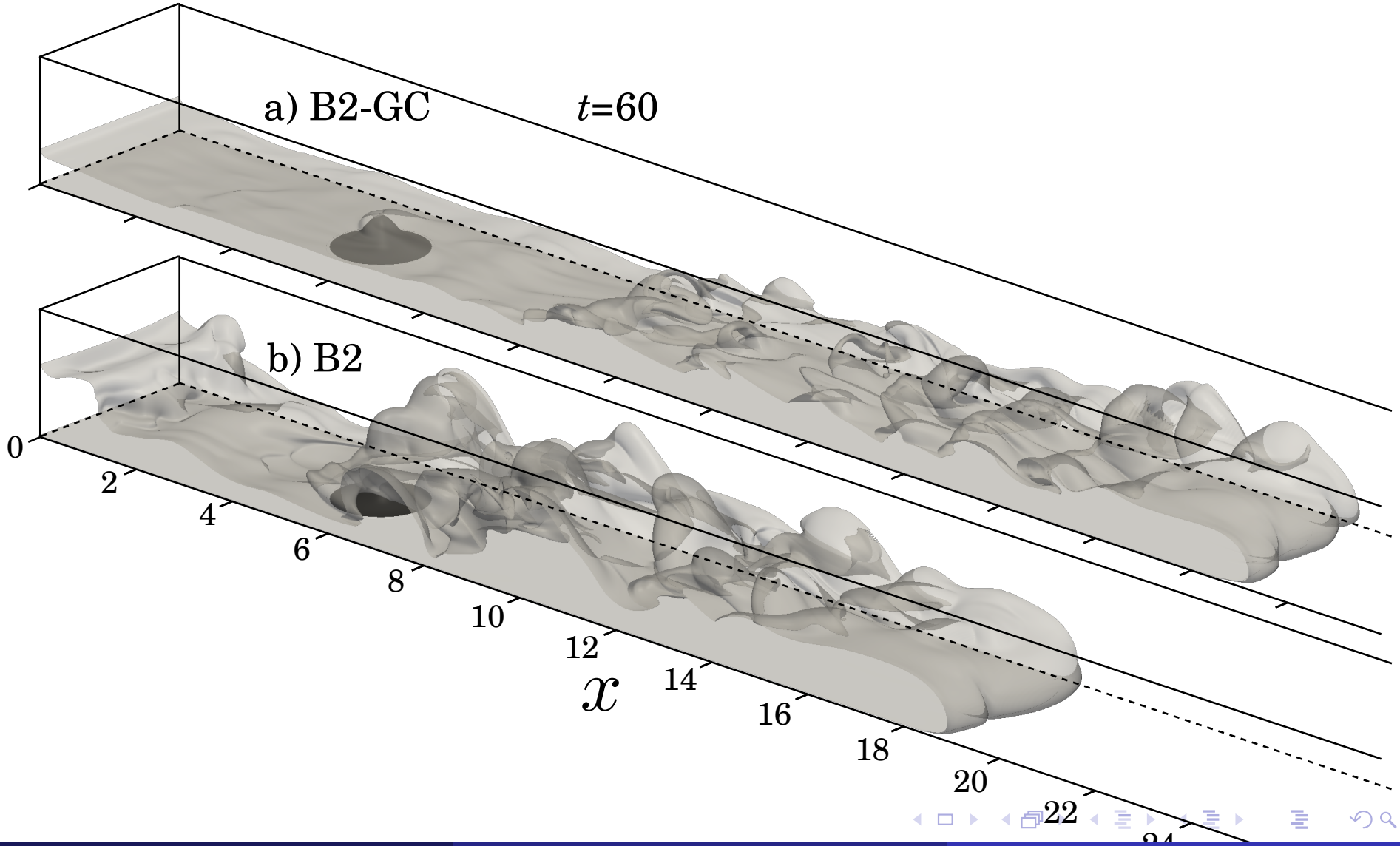

Results: Gravity vs turbidity current

Stronger stratification effects across the current height in case B2-GC

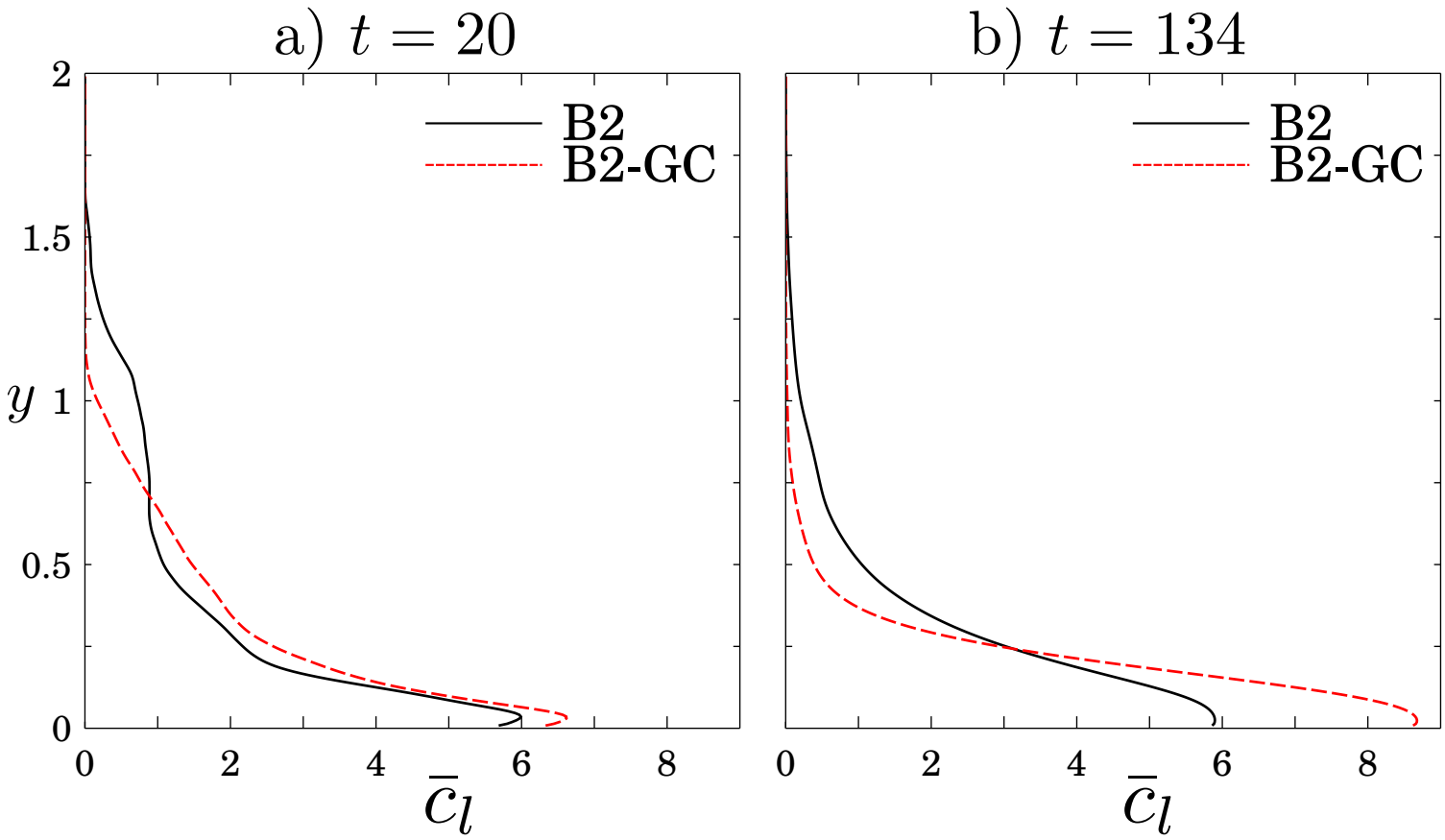

Results: Influence of Reynolds number

B2-GC case at $Re = 2,000$ and $Re = 5,000$. Initial 2D-strucutres demonstrate similar behavior

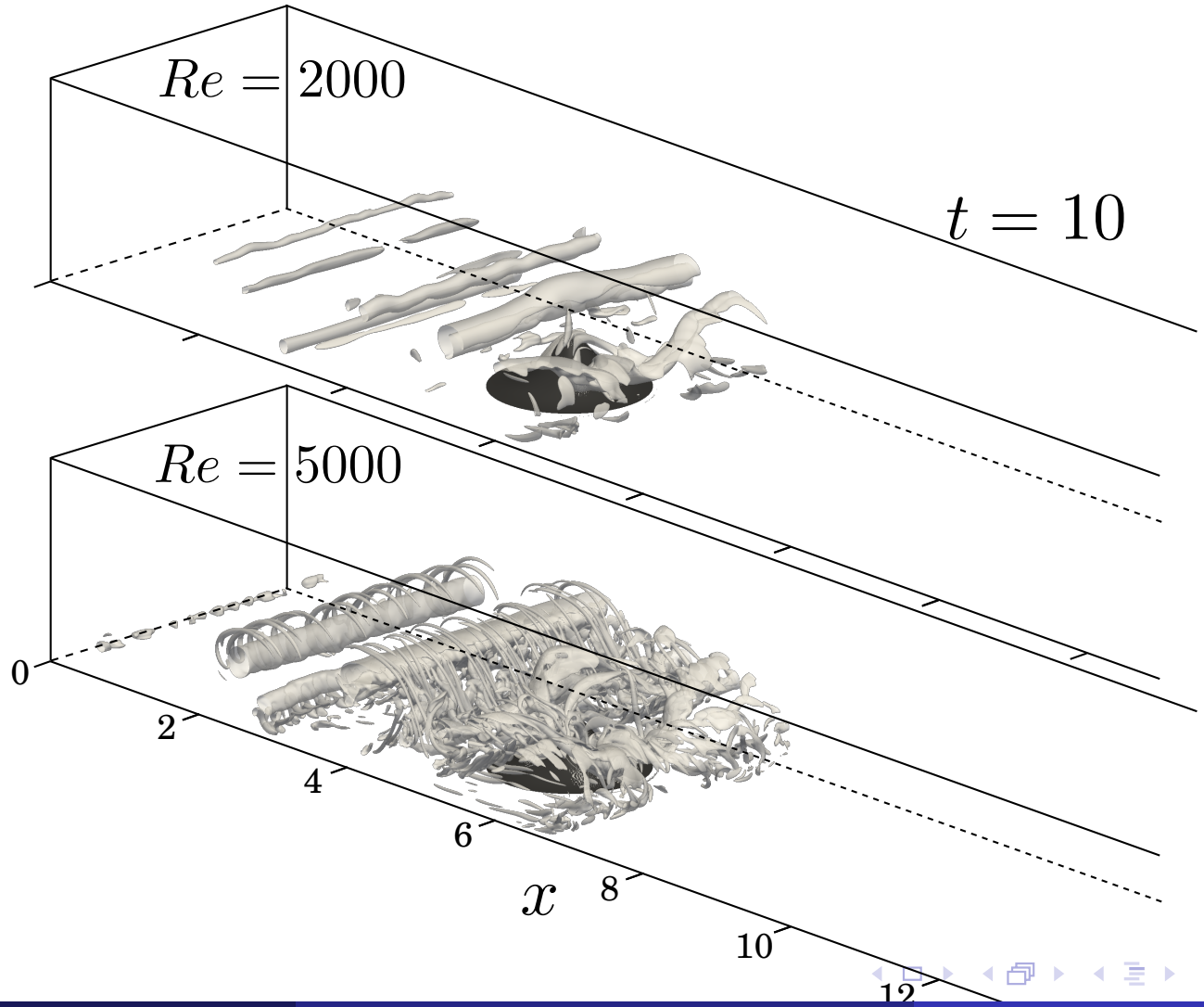

Results: Influence of Reynolds number

B2-GC case at $Re = 2,000$ and $Re = 5,000$. Production of fine scales after the interaction of the current with the bump

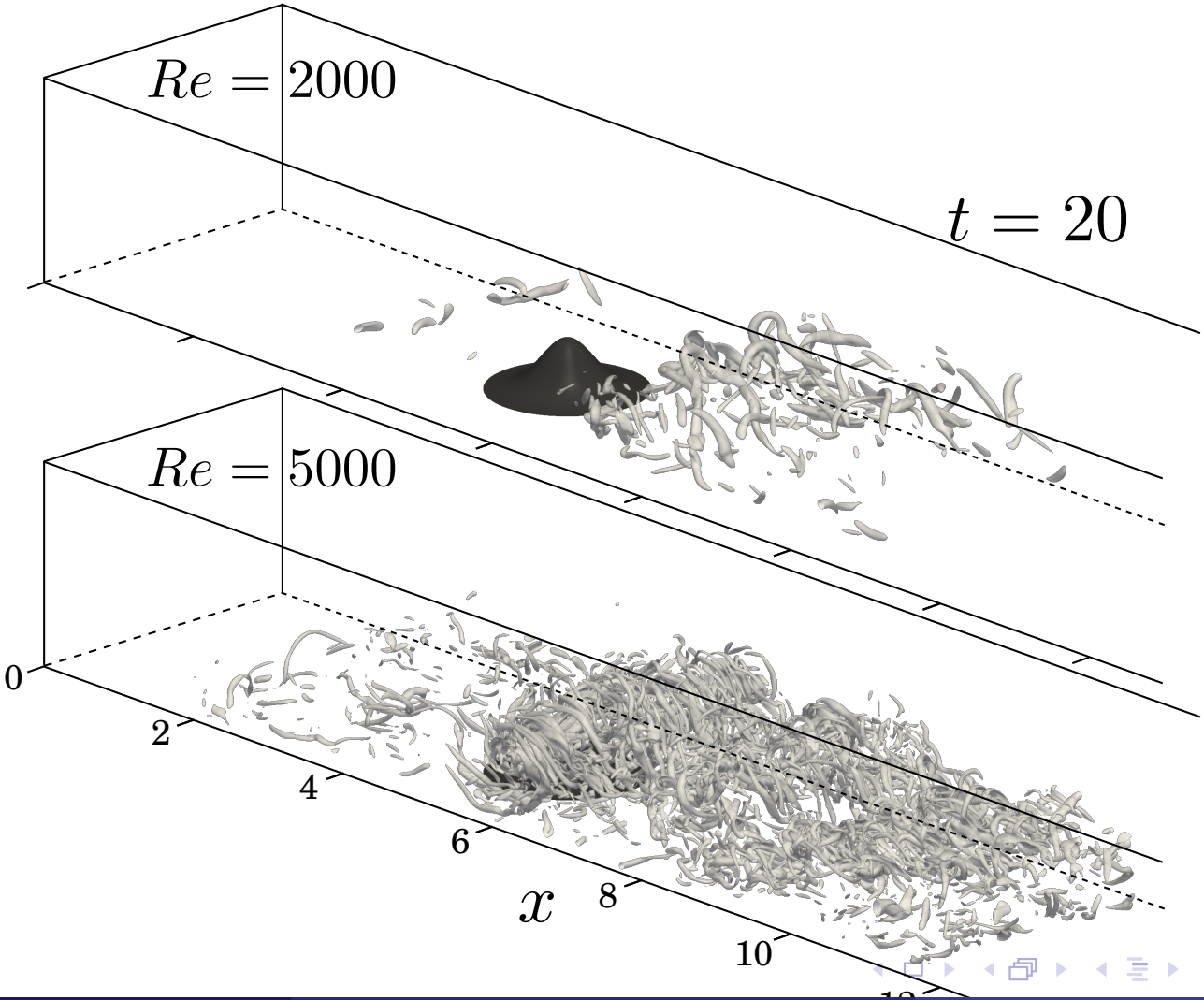

Results: Influence of Reynolds number

Influence on the lobe-and-cleft structures

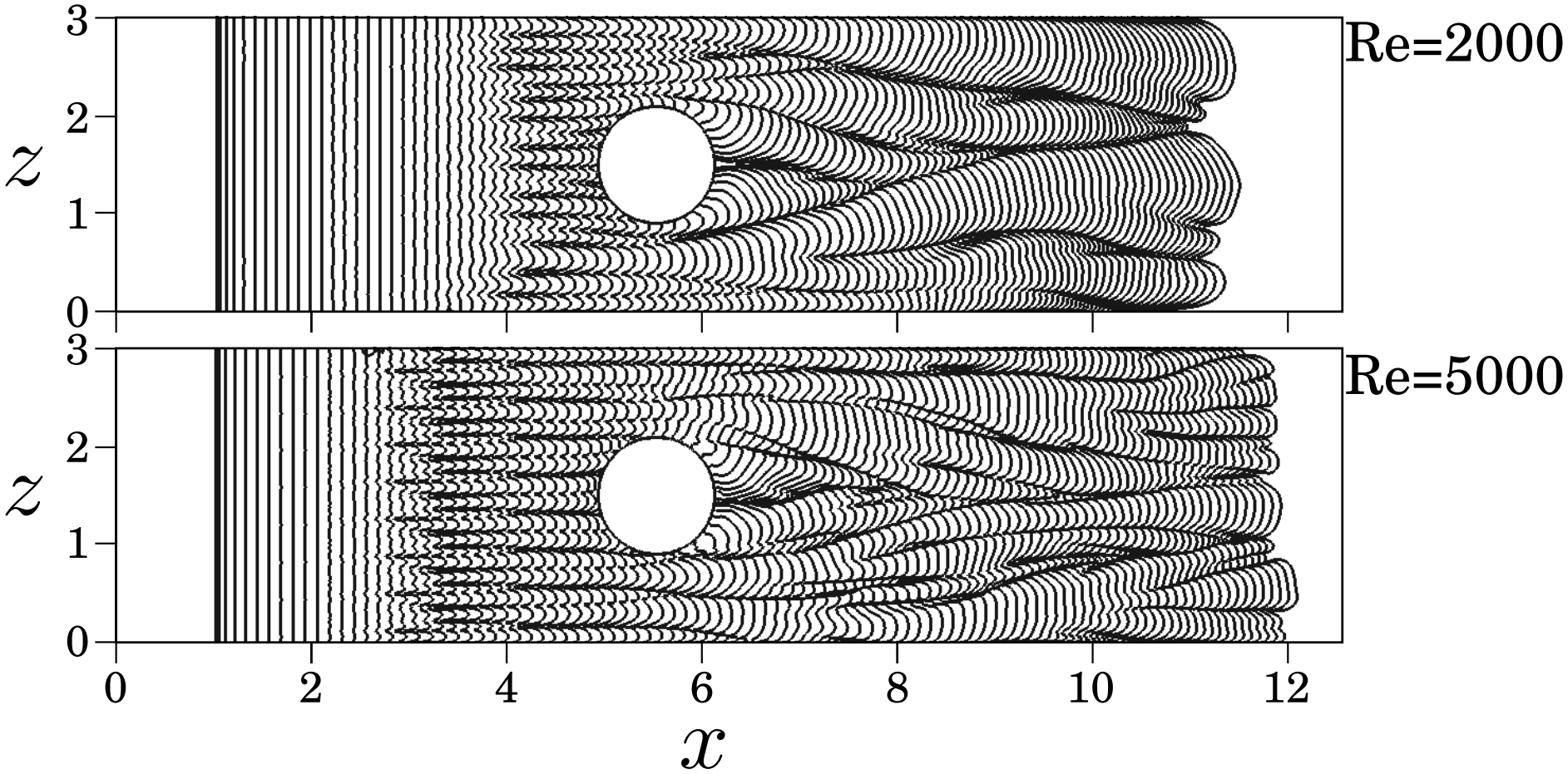

Results: Influence of Reynolds number

$Re = 5000$: increase in dilute mixing of interstitial and ambient fluid

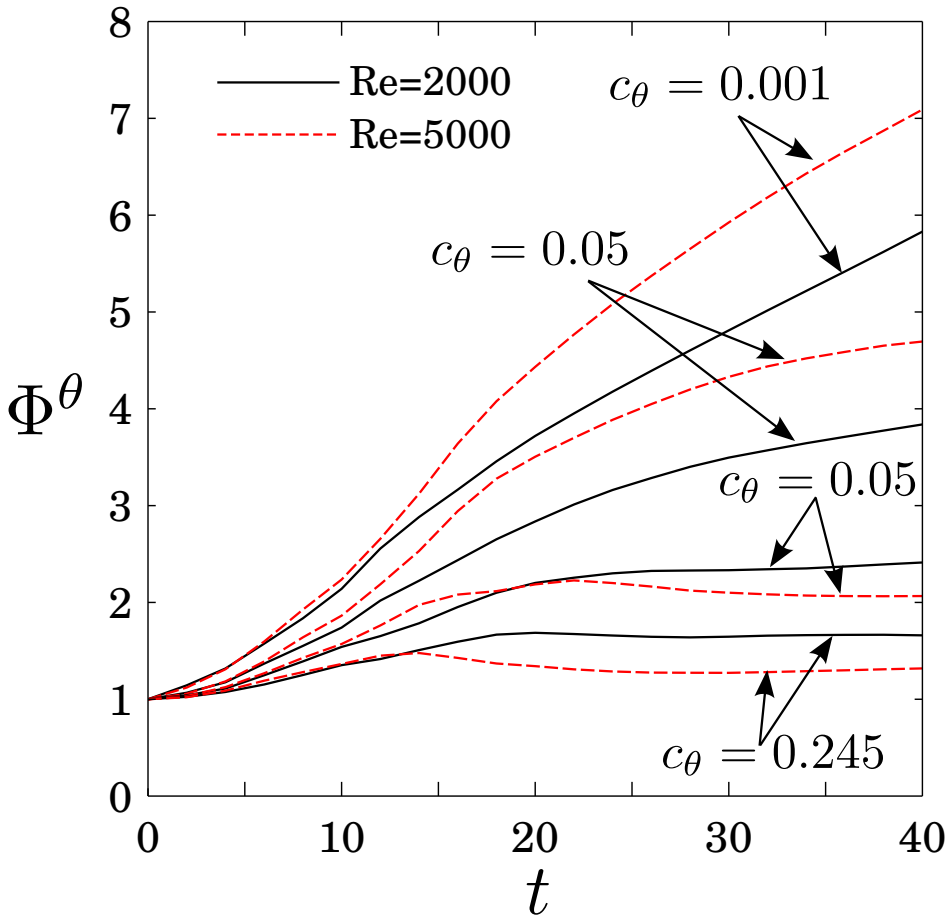

Results: Deposition

D^i_∞: final deposit height coarse ($i = 1$) and fine particles ($i = 2$).

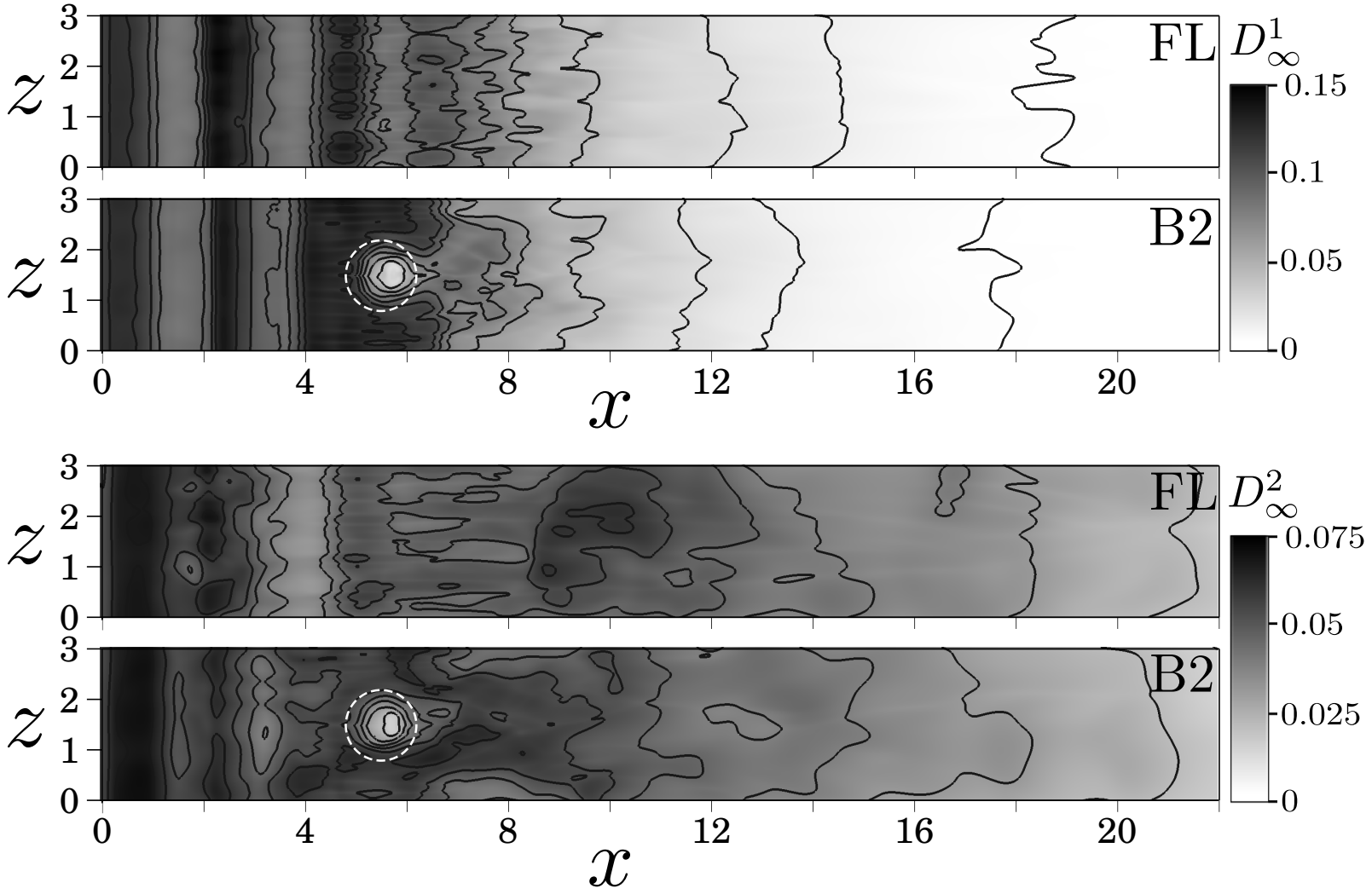

Results: Deposition

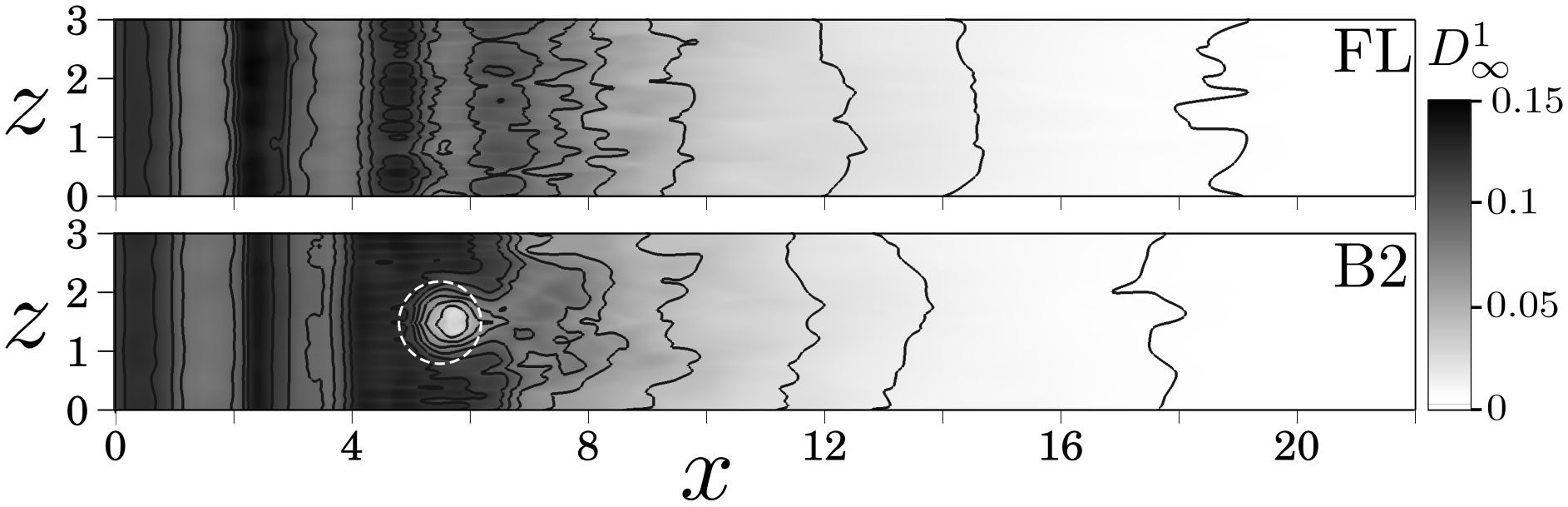

Results: Deposition

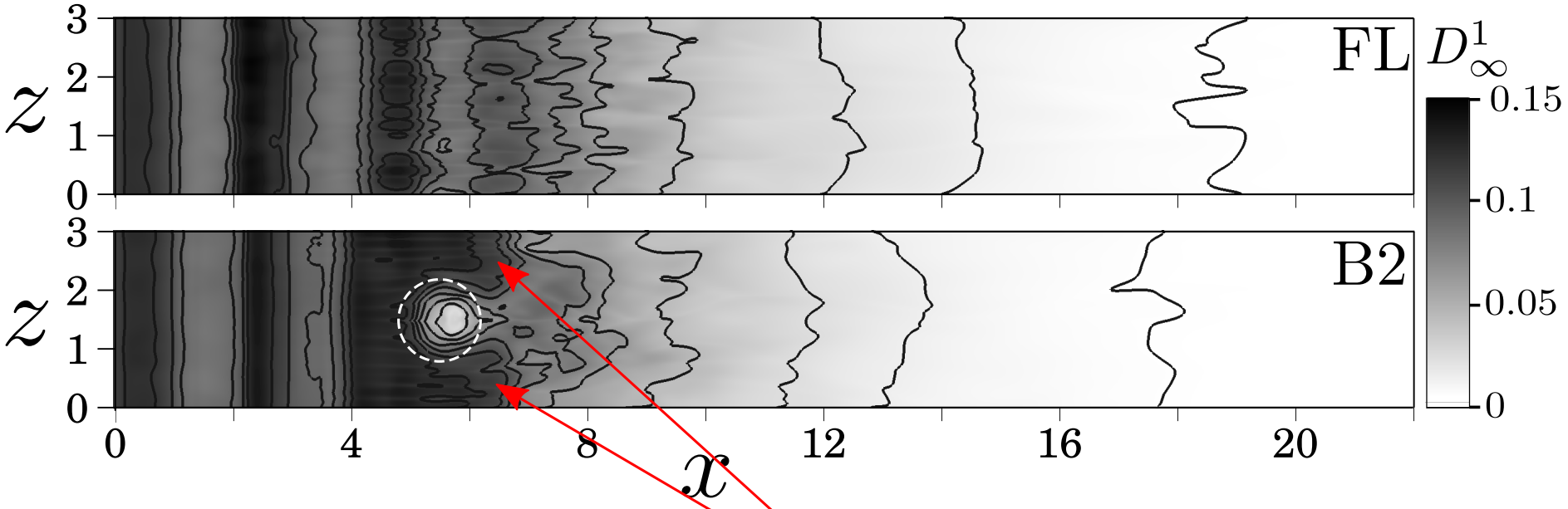

Lobe shaped profiles
due to lateral deflection

Results: Deposition

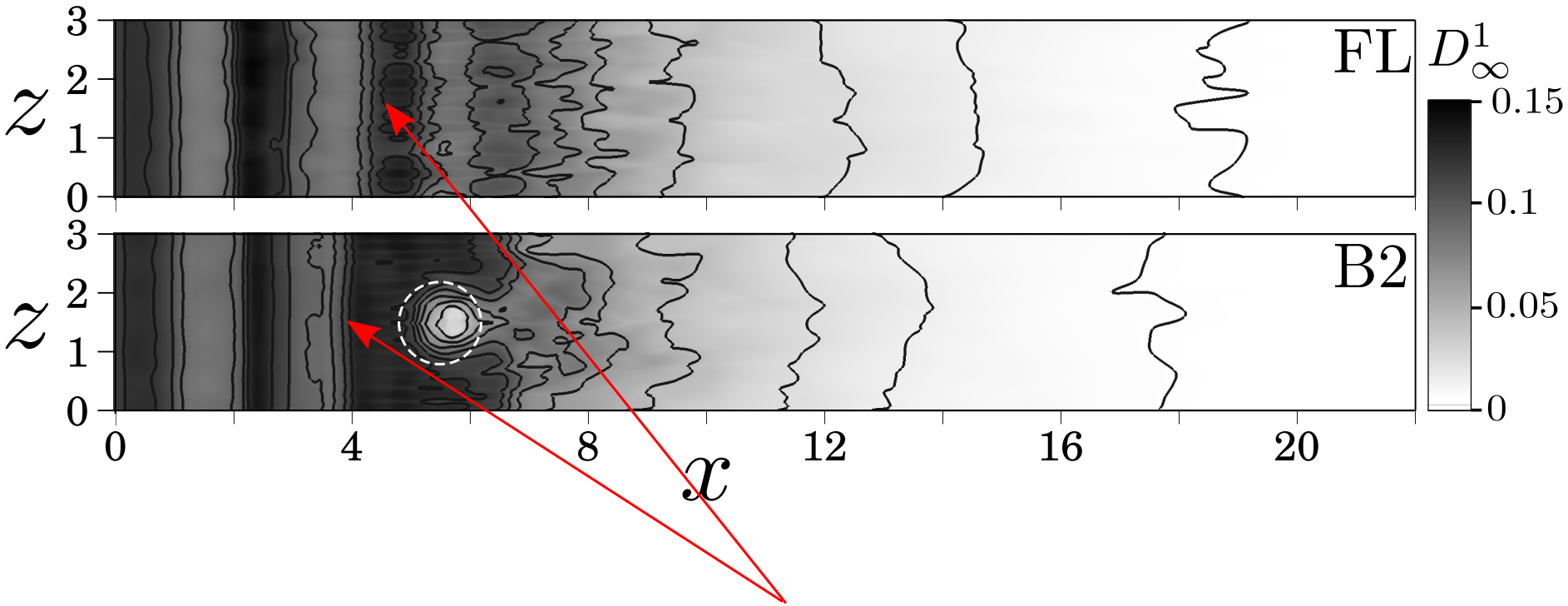

Increase in deposition due to flow deceleration and blocking effects

Results: Deposition

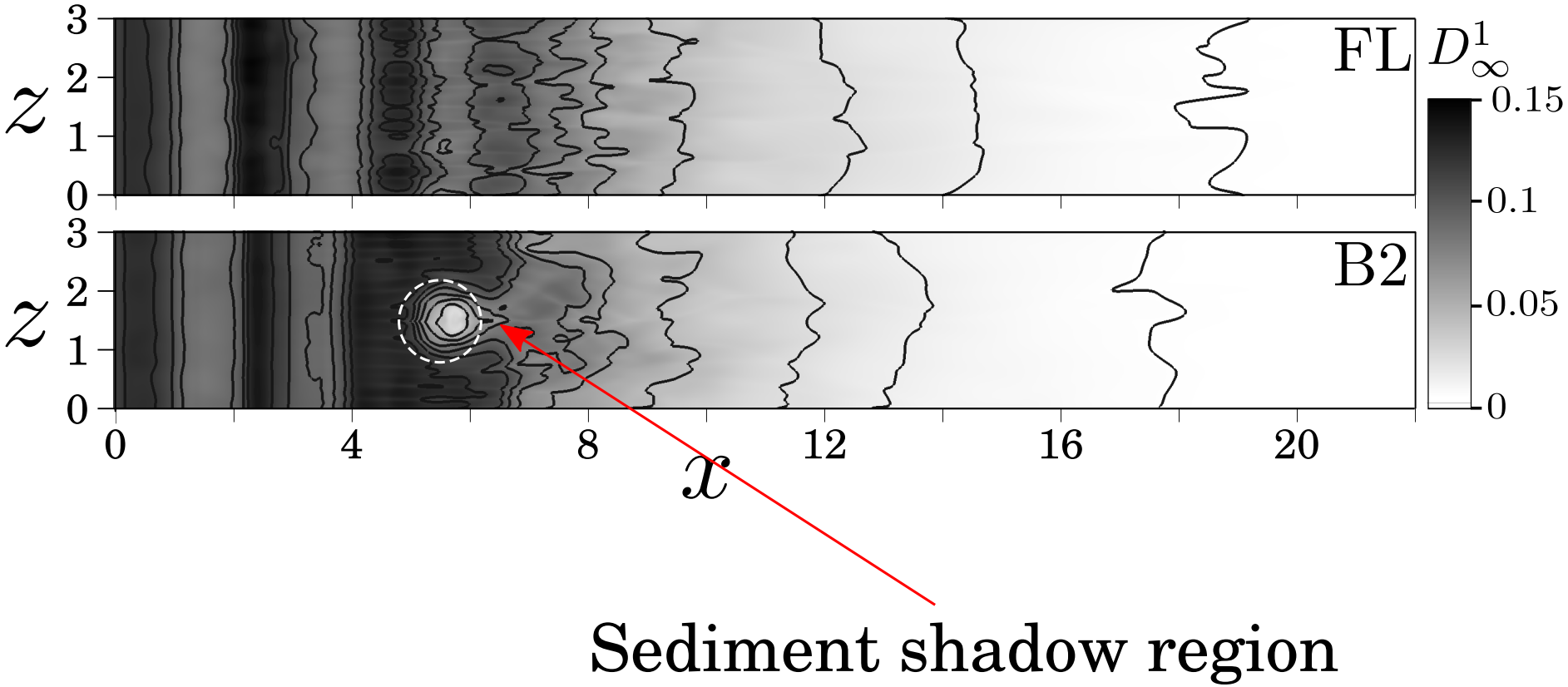

Results: Deposition

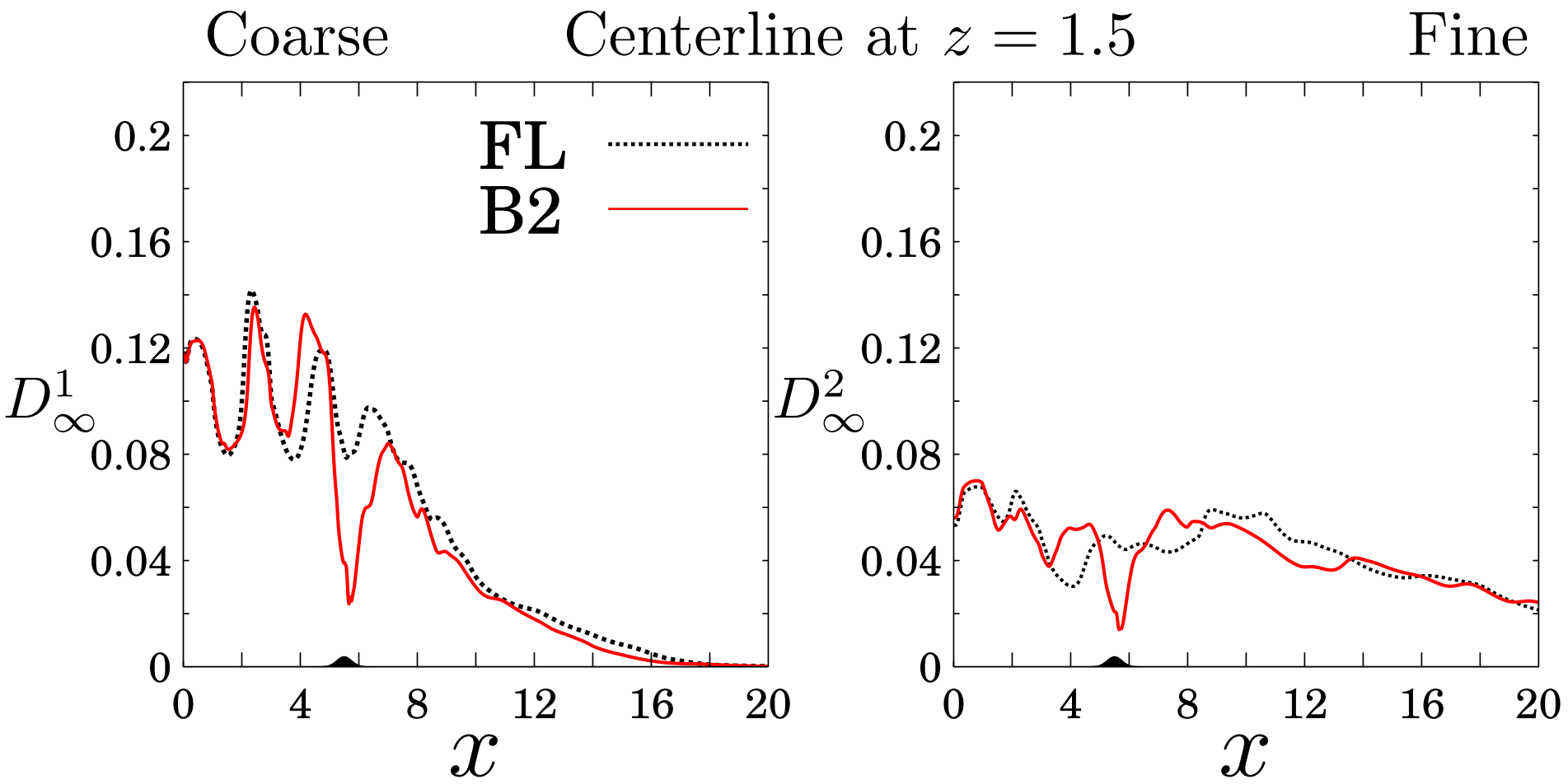

Results: Deposition

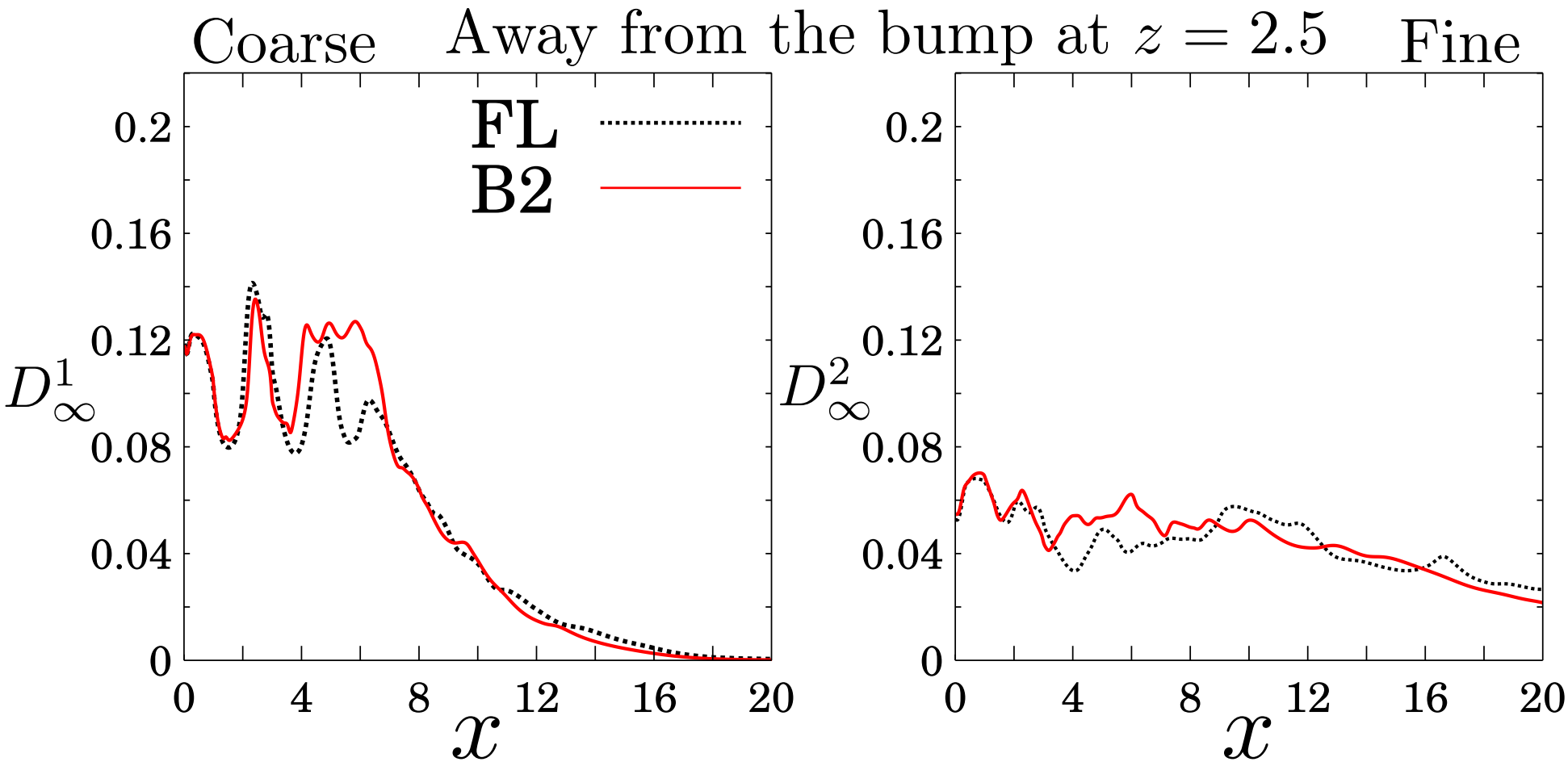

Results: Fate of particles

Question: Where do particles belonging to different regions in the lock settle out?

Question: How will mixing influence particles belonging to different horizontal subvolumes?

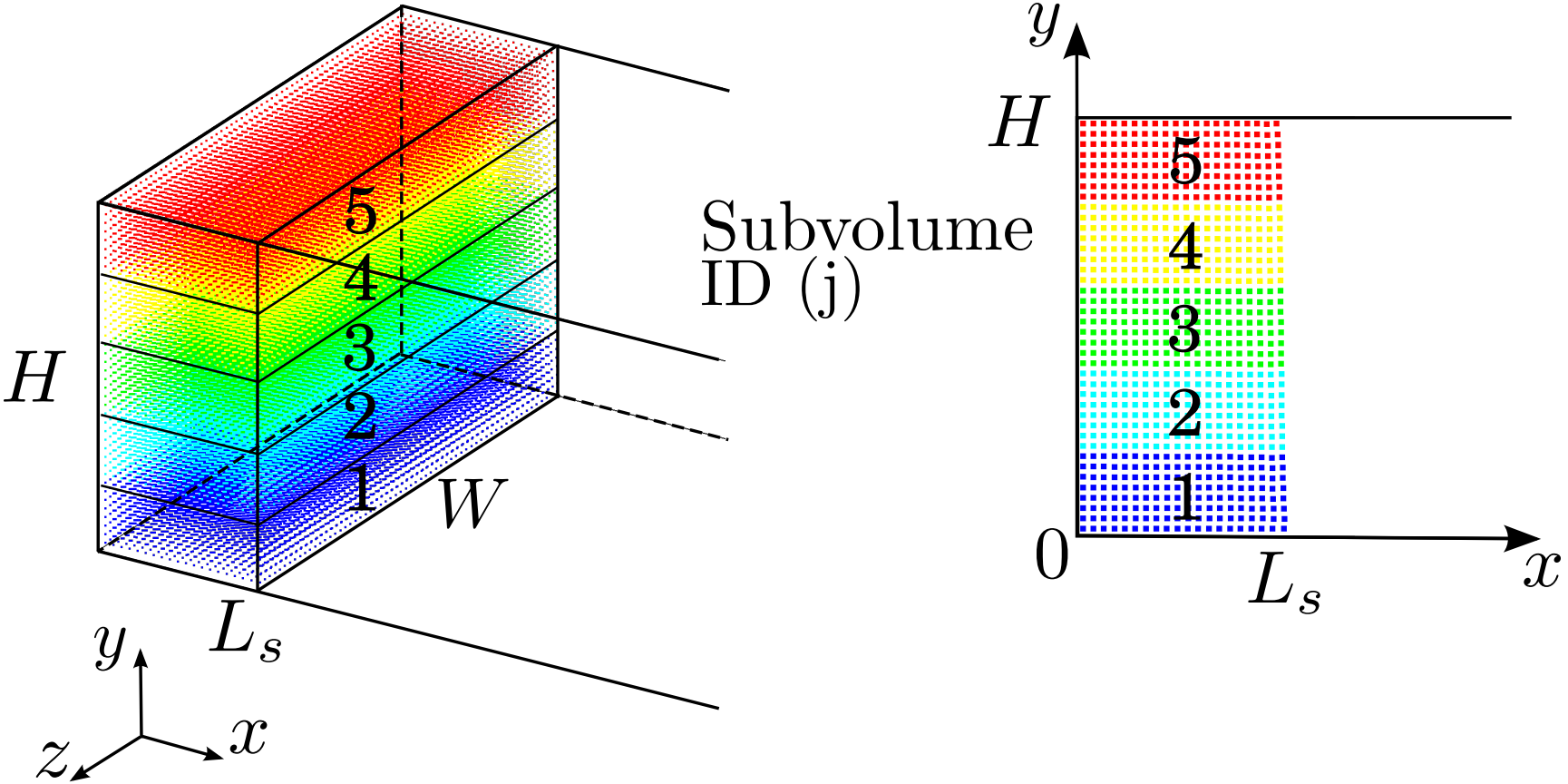

Results: Fate of particles

- 48,000 Largrangian markers
- Five subvolumes

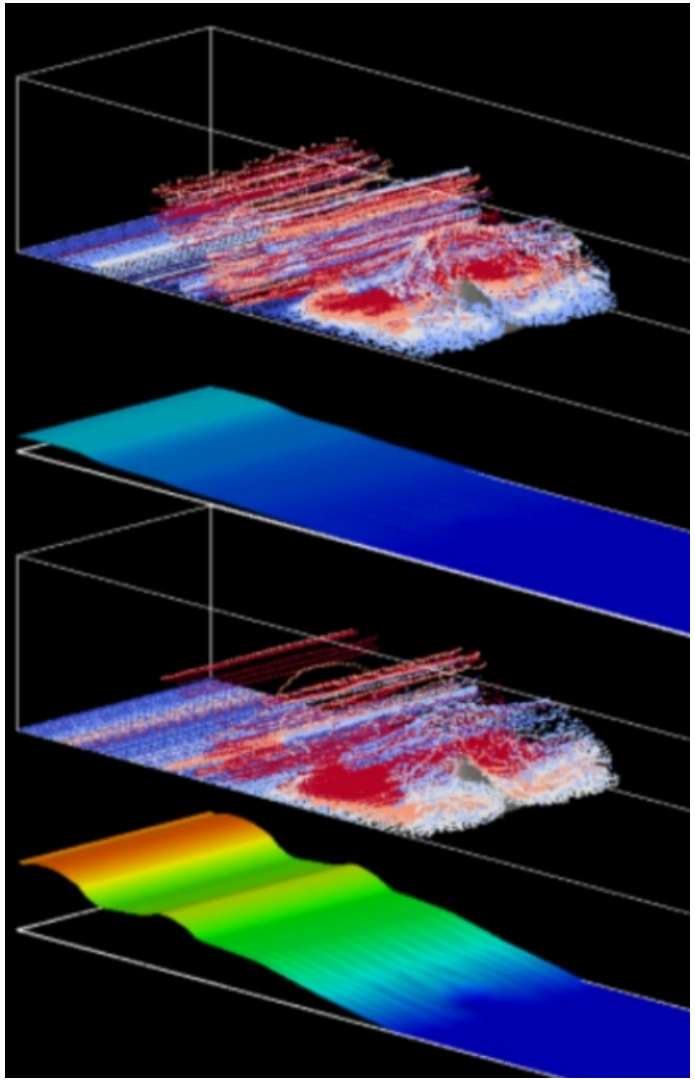

Results: Mixing of particles

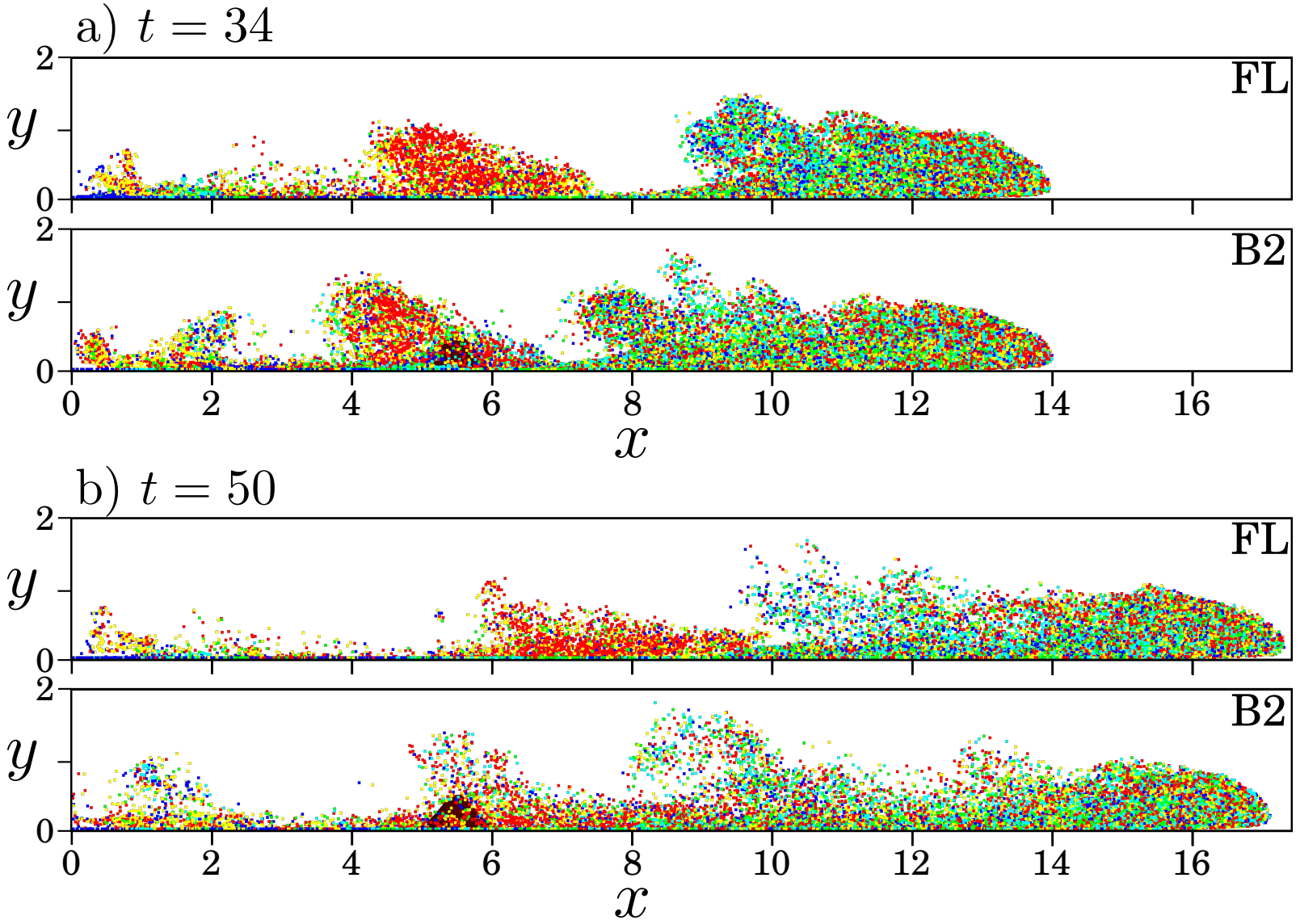

Results: Mixing of particles

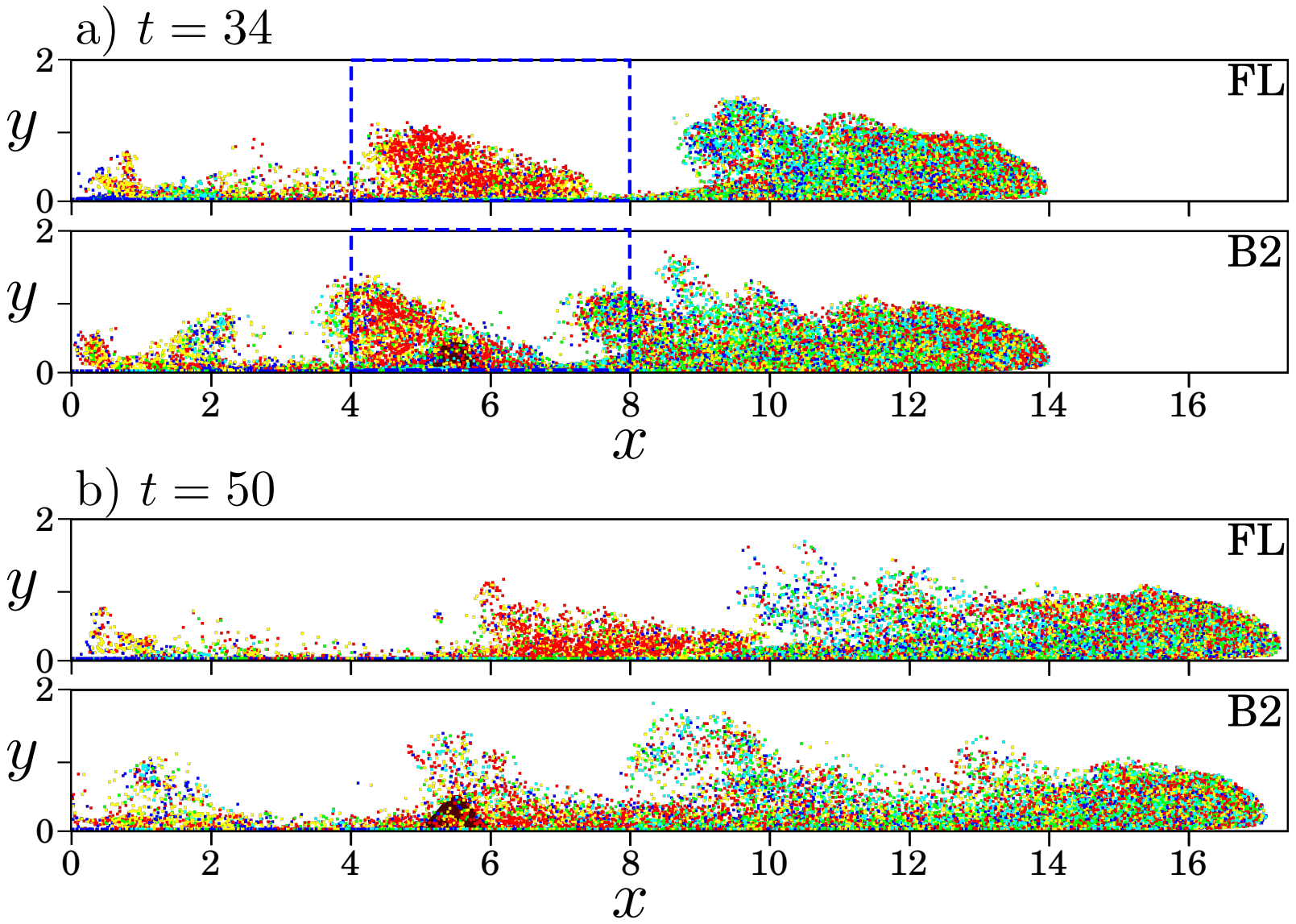

Results: Particle population in the vicinity of the bump

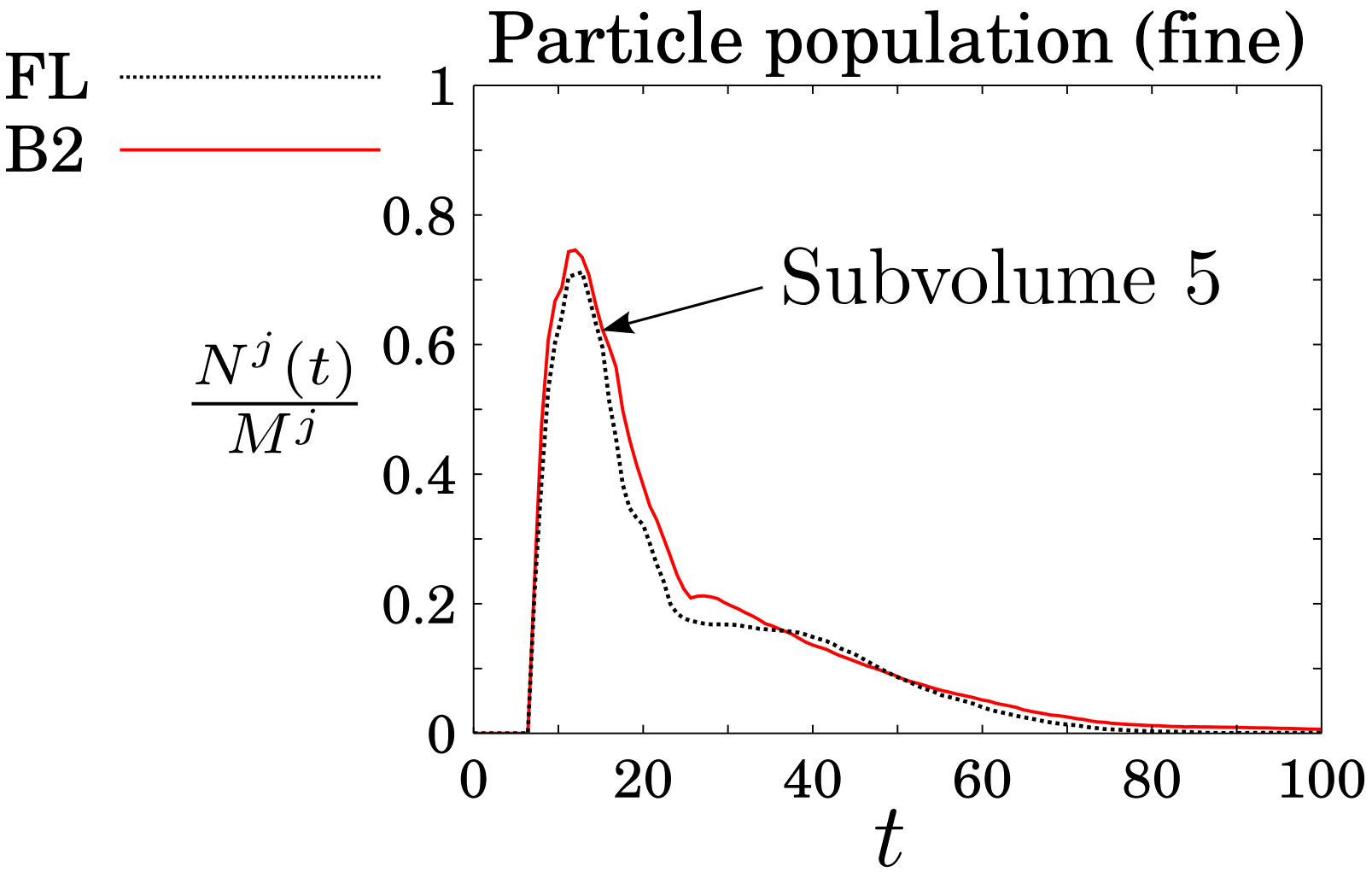

Results: Fate of coarse particles

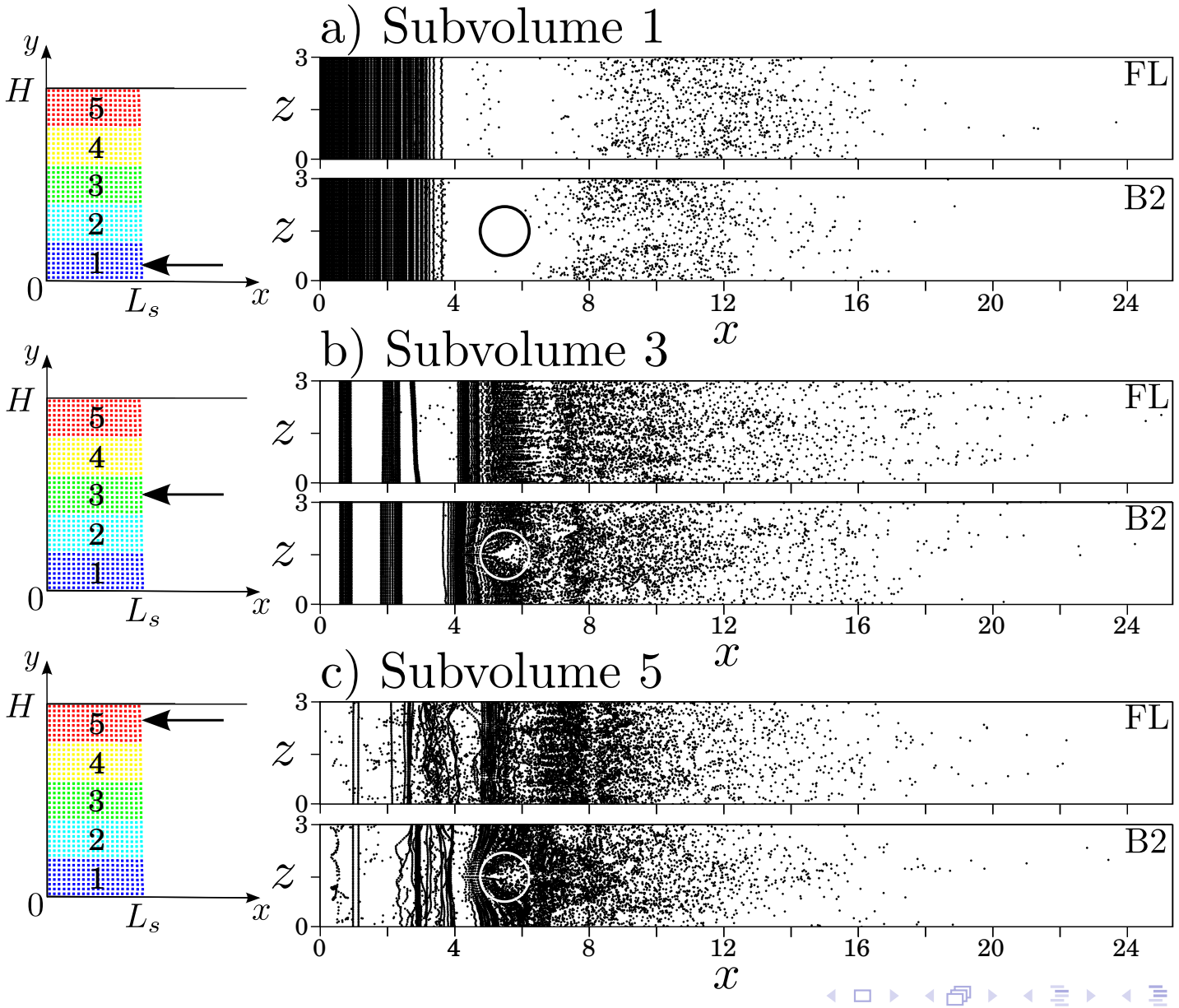

Results: Fate of fine particles

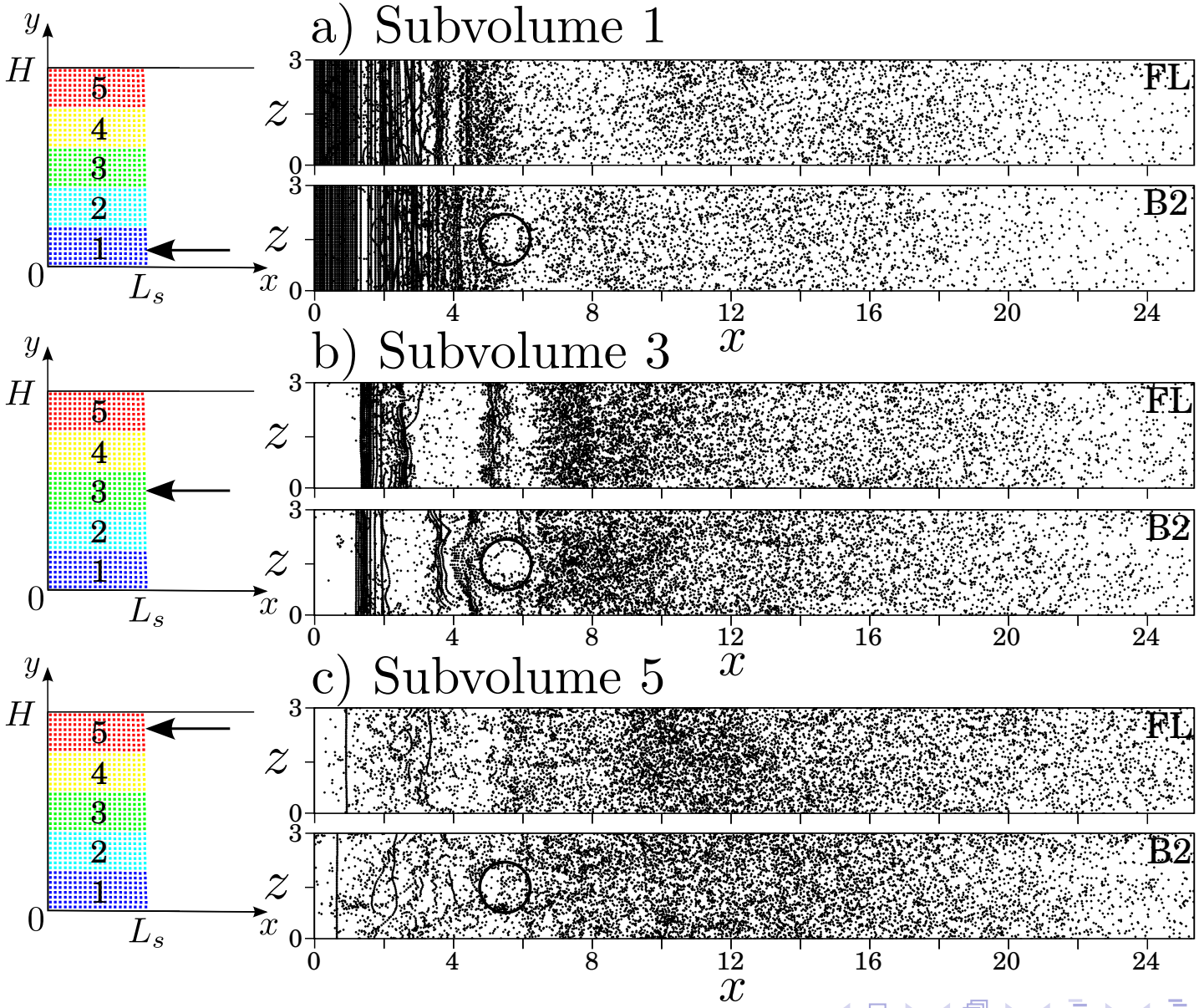

Results: Runout length

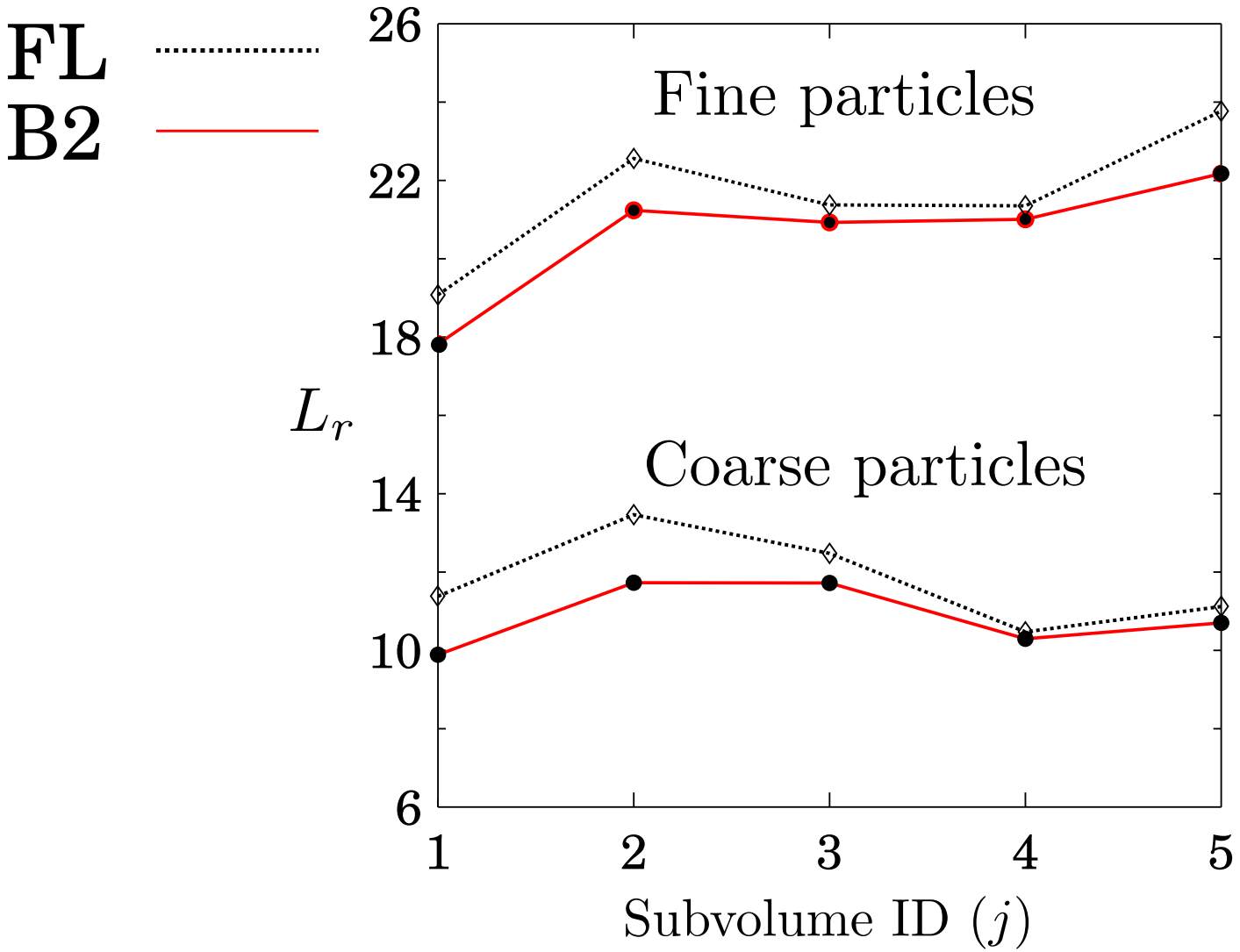

Summary

- We investigated the influence of two Gaussian bumps on various current properties
- Observation of a non-monotonic influence of the bump height on front location
- Initial enhanced mixing and dissipation in case B2 with the tallest bump
- Intermediate bump height (case B1) travels fastest and has stronger mixing during laters stages
- We investigated the mixing properties of the current as it travels over the bumps
- We employed Lagrangian markers to investigate the evolution and fate of the particles based on their origins in the lock

Acknowledgments

- Professor Ben Kneller: Insightful discussions on turbidity currents
- Funding: Prof. Ben Kneller's group from BG Group, BP, ConocoPhillips, DONG, GDF Suez, Hess, Petrobras, RWE Dea, Total, and Statoil.
- Computational time: Janus, Beach and Epic supercomputing facilities in CU Boulder, Colorado and UWA in Perth, Australia.

Movies

Movies are available at our youtube channel:

http://www.youtube.com/user/CFDLabUCSB

Publications

- M. M. Nasr-Azadani and E. Meiburg, *Influence of seafloor topography on the depositional behavior of bi-disperse turbidity currents: A three-dimensional, depth-resolved numerical investigation*, Accepted for Publication in Journal of Environmental Fluid Mechanics.

- M. M. Nasr-Azadani, B. Hall, E. Meiburg, (2013). *Polydisperse turbidity currents propagating over complex topography: Comparison of experimental and depth-resolved simulation results*. Computers & Geosciences 53 (0), 141-153.

- M. M. Nasr-Azadani and E. Meiburg, 2011. *TURBINS: An immersed boundary, Navier-Stokes code for the simulation of gravity and turbidity currents interacting with complex topographies*. Computers & Fluids 45 (1), 14-28.

- M. M. Nasr-Azadani and E. Meiburg, *Turbidity currents interacting with three-dimensional seafloor topography*, Submitted to Journal of Fluid Mechanics.